

CHAPTER IV

RESULTS AND DISCUSSION

4.1 Characterization

4.1.1 UV-Visible spectroscopy

UV-VIS spectra were measured to illustrate the optical properties of conductive polymers. The optical properties of conductive polymers were considered in terms of absorption wavelength, which was converted to photon energy in electron volt units by using Einstein's equation as shown in Equation 3.1.

The UV-VIS spectrum of undoped polyaniline (emeraldine base) solution at the concentration 0.1 g/l. is shown in Figure 4.1. It shows two absorption peaks at 325 and 625 nm due to the π - π^* transition of benzenoid ring and the exciton absorption of quinoid ring, respectively (Chen *et al.*, 1995).

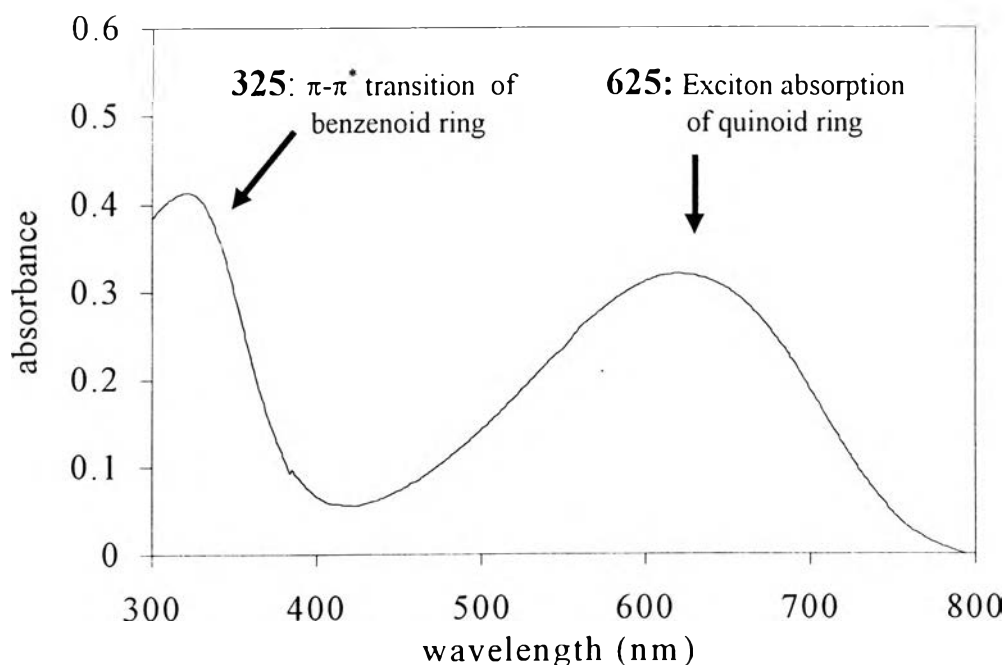


Figure 4.1 UV-VIS spectrum of undoped polyaniline (emeraldine base).

To study the effect of dopant types and acid/polymer concentration ratios on the electrical conductivity, the polyaniline emeraldine base was doped with different acid dopant types and the acid/polymer concentration ratio was varied in each dopant. Figures 4.2–4.5 show the UV-VIS spectra of polyaniline emeraldine base doped with various acid dopants; HCl, H₃PO₄, CH₃COOH and C₅H₁₁COOH. After doping, N atoms on imine groups were protonated, N and its neighboring quinoid ring became semiquinoid radical cations (Furukawa *et al.*, 1988). This caused a decrease in the exciton absorption peak intensity at 625 nm and generating two new absorption peaks at 420 and 865 nm corresponding to the presence of polaron/ bipolaron states, indicative the conducting behavior of the polymer (Chen and Lin *et al.*, 1995). For strong acids, HCl and H₃PO₄, the polaron/ bipolaron states were present at lower acid/polymer concentration ratios relative to the weak acids; CH₃COOH and C₅H₁₁COOH, depending on pK_a as shown in Table 4.1. Both HCl and H₃PO₄ have lower pK_a indicating that they have higher efficiencies to protonate H⁺ on the polymer chains and the polaron/bipolaron states can be formed at very low acid/polymer concentration ratios.

Table 4.1 Shows the acid dissociation constant (pK_a) of various acids in water at 25°C (John, 1987)

Acids	Acid dissociation constant (pK _a)
HCl	-6.10
H ₃ PO ₄	pK _{a1} = 2.15, pK _{a2} = 5.10
CH ₃ COOH	4.76
C ₅ H ₁₁ COOH	4.85

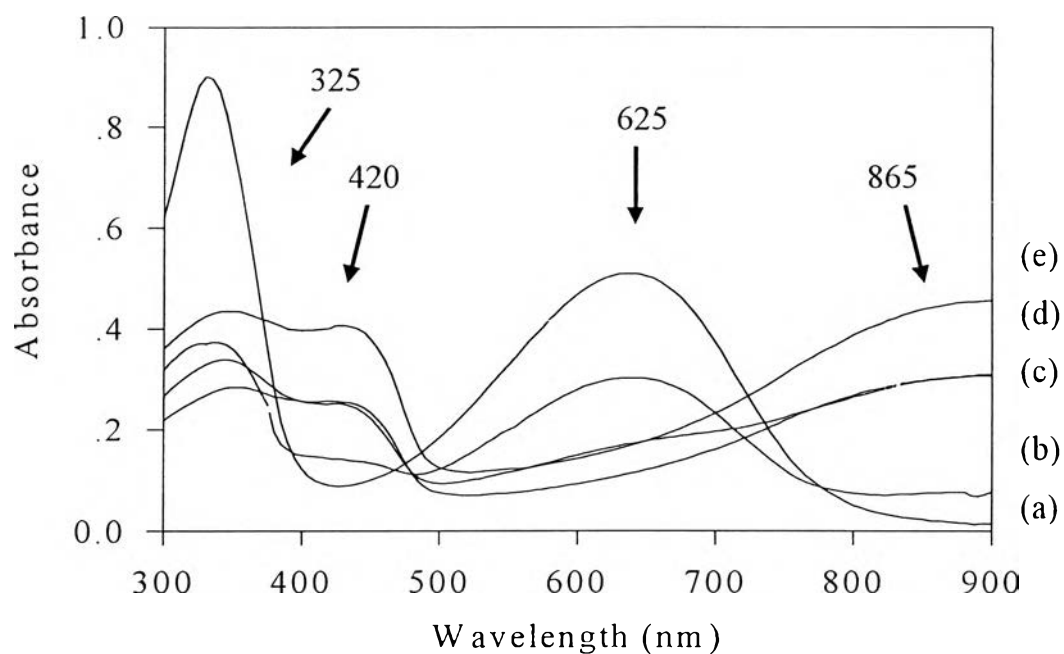


Figure 4.2 UV-VIS spectra of HCl-doped polyaniline at C_a/C_p of (a) 1:1 ($N_a/N_p=9.8E+00$), (b) 1.5:1 ($N_a/N_p=1.45E+01$), (c) 1.7:1 ($N_a/N_p=1.6E+01$), (d) 1.9:1 ($N_a/N_p=1.9E+01$), and (e) 2:1 ($N_a/N_p=2.0E+01$).

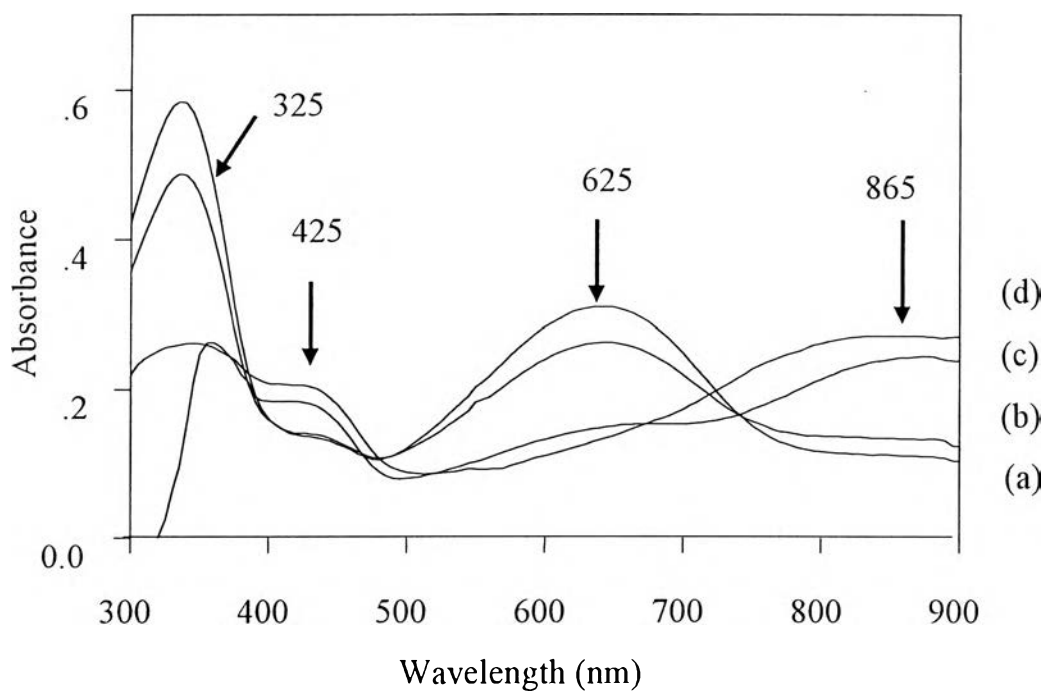


Figure 4.3 UV-VIS spectra of H_3PO_4 -doped polyaniline at C_a/C_p of (a) 15:1 ($N_a/N_p=5.5E+01$), (b) 20:1 ($N_a/N_p=7.3E+01$), (c) 40:1 ($N_a/N_p=1.E+02$), and (d) 50:1 ($N_a/N_p=1.8E+02$).

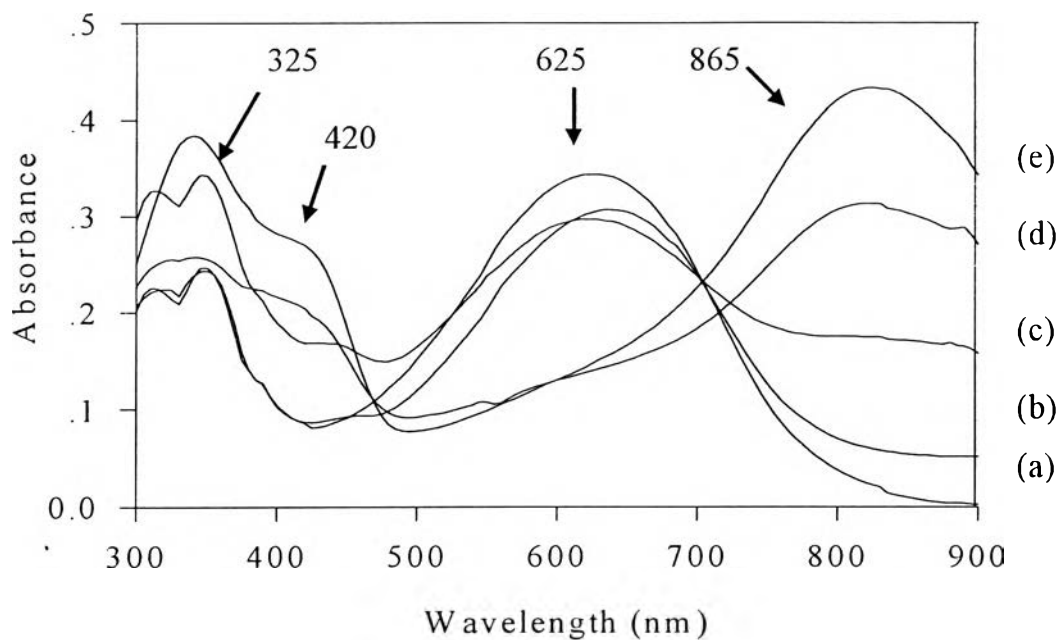


Figure 4.4 UV-VIS spectra of CH_3COOH -doped polyaniline at C_a/C_p of (a) 10000:1 ($N_a/N_p=5.9\text{E}+04$), (b) 15000:1 ($N_a/N_p=8.9\text{E}+04$), (c) 20000:1 ($N_a/N_p=1.1\text{E}+05$), (d) 30000:1 ($N_a/N_p=1.8\text{E}+05$), and (e) 40000:1 ($N_a/N_p=2.2\text{E}+05$).

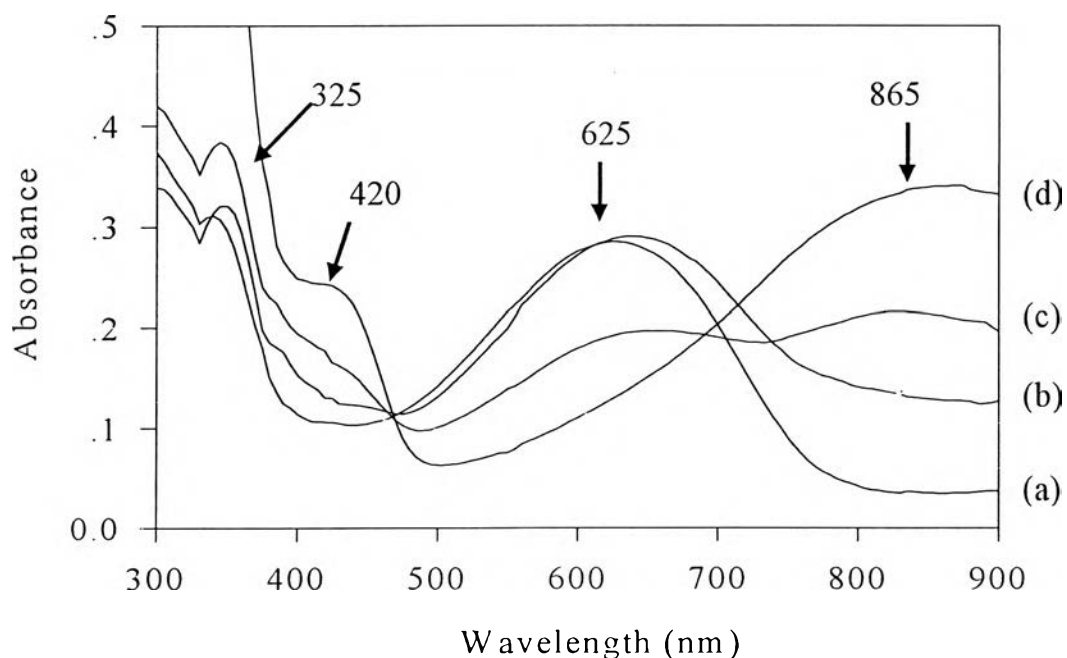


Figure 4.5 UV-VIS spectra of $\text{C}_3\text{H}_{11}\text{COOH}$ -doped polyaniline C_a/C_p of (a) 30000:1 ($N_a/N_p=9.2\text{E}+04$), (b) 40000:1 ($N_a/N_p=1.2\text{E}+05$), (c) 45000:1 ($N_a/N_p=1.4\text{E}+05$), and (d) 50000:1 ($N_a/N_p=1.5\text{E}+05$).

Table 4.2 The assignment for UV-Visible absorption peaks of polyaniline emeraldine base and doped-polyaniline (MacDiarmid and Epstein, 1989)

Wavelength (nm)	Assignment
325	π - π^* transition of benzenoid ring
420	Bipolaron state
625	π - π^* transition of quinoid ring
865	Polaron state

4.1.2 FT-IR Spectroscopy.

The FT-IR spectrum of polyaniline emeraldine base (undoped state) is shown in Figure 4.6

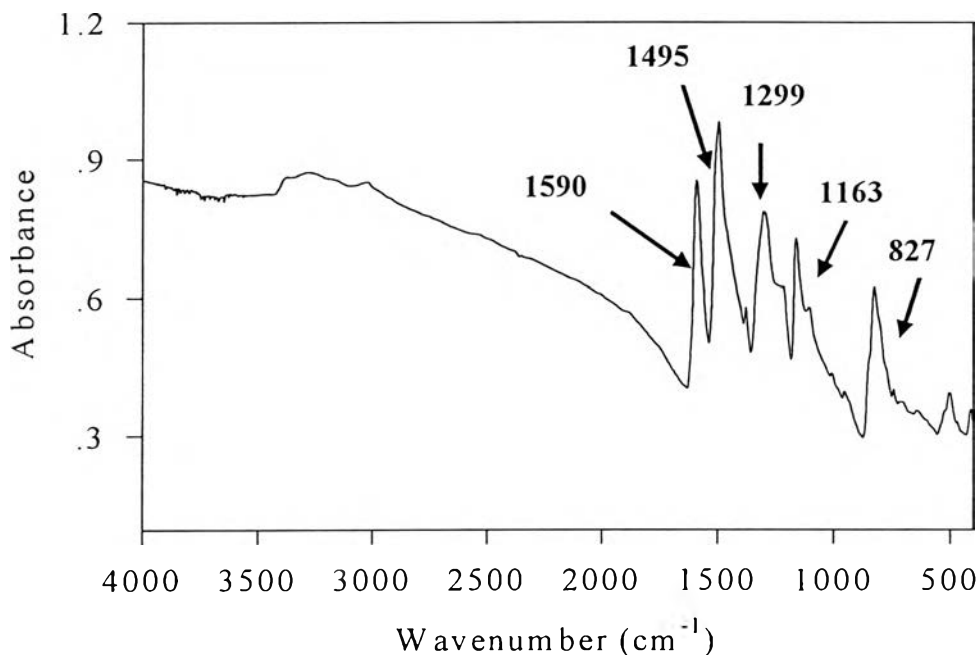


Figure 4.6 The FT-IR spectrum of polyaniline emeraldine base film.

The spectrum of emeraldine base shows 5 important absorption bands. At 1590 cm^{-1} , it represents the C=N stretching of quinoid ring, $\text{—}\ddot{\text{N}}=\text{C}_6\text{H}_4=\ddot{\text{N}}\text{—}$. The band and at 1495 cm^{-1} indicates the stretching of benzenoid ring, $\text{—}\ddot{\text{N}}\text{H}-\text{C}_6\text{H}_4-\ddot{\text{N}}\text{H}\text{—}$. The C-N stretching of benzenoid ring can be observed at 1299 cm^{-1} . The band at 1163 cm^{-1} refers to in-plane C-H bending motion of quinoid ring and the band at 827 cm^{-1} identifies out of plane bending of C-H bond in aromatic ring (Milton and Monkman, 1993).

Table 4.3 Assignment for IR absorption bands for polyaniline emeraldine base (Milton and Monkman, 1993)

Wavenumber (cm ⁻¹)	Assignment
1590	C=N stretching of quinoid ring
1495	Stretching of benzenoid ring
1299	C-N stretching of benzenoid ring
1163	In-plane C-H bending of quinoid ring
827	Out of plane bending of 1,4-ring

Figures 4.7- 4.10 show the FT-IR spectra of polyaniline films doped with HCl, H₃PO₄, CH₃COOH and C₅H₁₁COOH at various acid/polymer concentration ratios. For polyaniline films doped with HCl, new bands at 1735, 1154, 1054, 1014 and 854 cm⁻¹ can be observed. The band at 1735 cm⁻¹ represents the C=O stretching of NMP in polyaniline films (Wei *et al.*, 1992). The band at 1154 cm⁻¹ indicates the broken symmetry mode of quinoid structure (Chan *et al.*, 1994). The band at 827 cm⁻¹ in emeraldine base was shifted to 854 cm⁻¹ after doping due to the change in quinoid structure to benzenoid structure (Zeng and Ko, 1998). At higher acid/polymer concentration ratios, the bands at 1054 and 1014 cm⁻¹ were present because of the substitution of excess chloride ions which compensated the positive charges on the benzenoid ring (Morales *et al.*, 1997).

When polyaniline emeraldine base was doped with phosphoric acid, the quinoid band was shifted downward from 1590 cm⁻¹ to 1643 cm⁻¹. The new bands at 1118 cm⁻¹ and 1006 cm⁻¹ indicate the vibration mode of P=O and phosphate anion (PO₄³⁻) of H₃PO₄, which stabilize the positive charges on the polymer chains (Chan *et al.*, 1994).

For the doping polyaniline emeraldine base with the weak acids, acetic acid and hexanoic acid, the IR spectra of doped polyaniline with

these two acids types were similar in both undoped and doped forms because the weak acids had less efficiency to protonate H^+ on polymer chains even at relatively high acid/polymer concentration ratio.

Table 4.4 Assignments for IR absorption band for doped polyaniline

Wavenumber (cm^{-1})	Assignments	References
2978	C-H stretching of alkyl group	Zeng and Ko, (1998)
1735	C=O stretching of NMP	Wei <i>et al.</i> , (1992)
1154	Broken symmetry mode of quinoid structure	Chan <i>et al.</i> , (1994)
1118	Vibration mode of P=O	Chan <i>et al.</i> , (1994)
1054	Cl ⁻ substitution on meta-position	Morales <i>et al.</i> , (1997)
1014	Cl ⁻ substitution on orthro- position	Morales <i>et al.</i> , (1997)
1006	Vibration mode of PO_4^{2-}	Chan <i>et al.</i> , (1994)
854	Out of plane bending of 1, 2, 4- aromatic ring	Zeng and Ko, (1998)

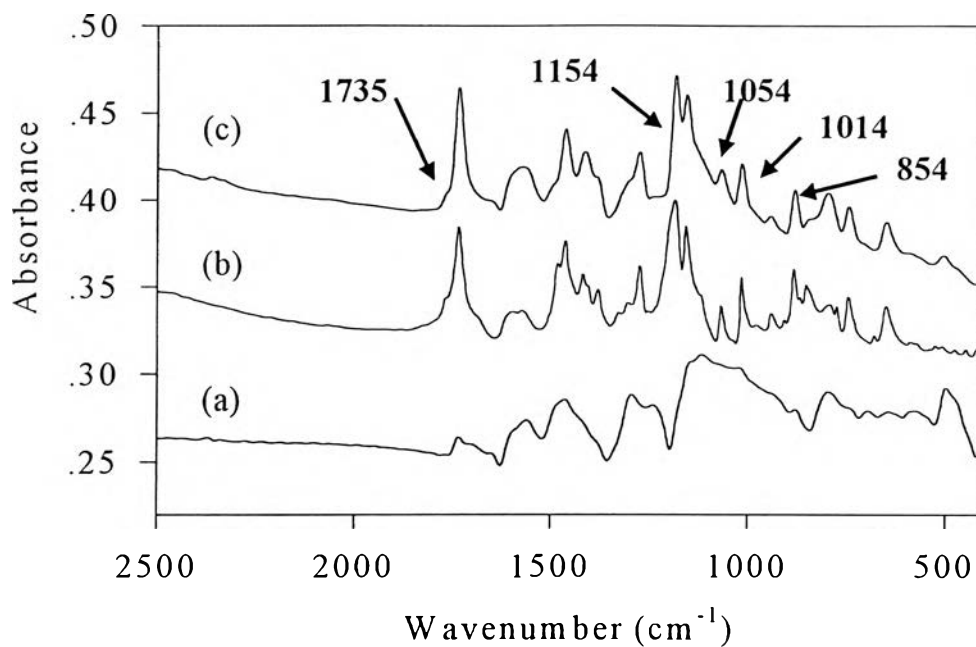


Figure 4.7 FT-IR spectra of HCl-doped polyaniline films at C_a/C_p of (a) 1:1 ($N_a/N_p=9.8E+00$), (b) 10:1 ($N_a/N_p=9.8E+01$), and (c) 500:1 ($N_a/N_p=4.9E+03$).

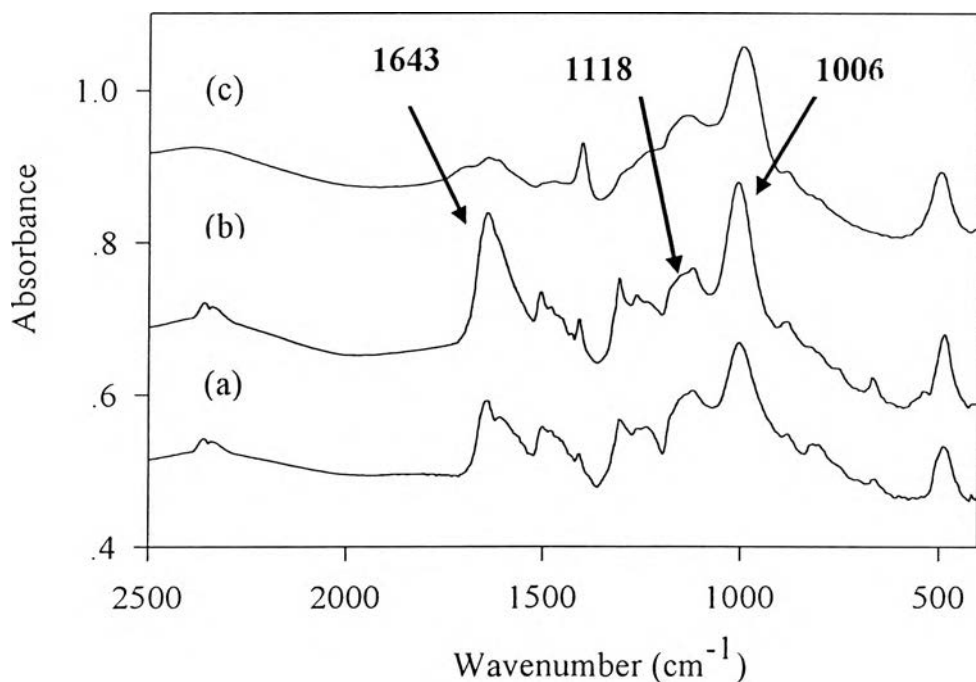


Figure 4.8 FT-IR spectra of H_3PO_4 doped-polyaniline films at C_a/C_p of (a) 1:10 ($N_a/N_p=3.6E-01$), (b) 1:1 ($N_a/N_p=3.6E+00$), and (c) 10:1 ($N_a/N_p=3.6E+01$).

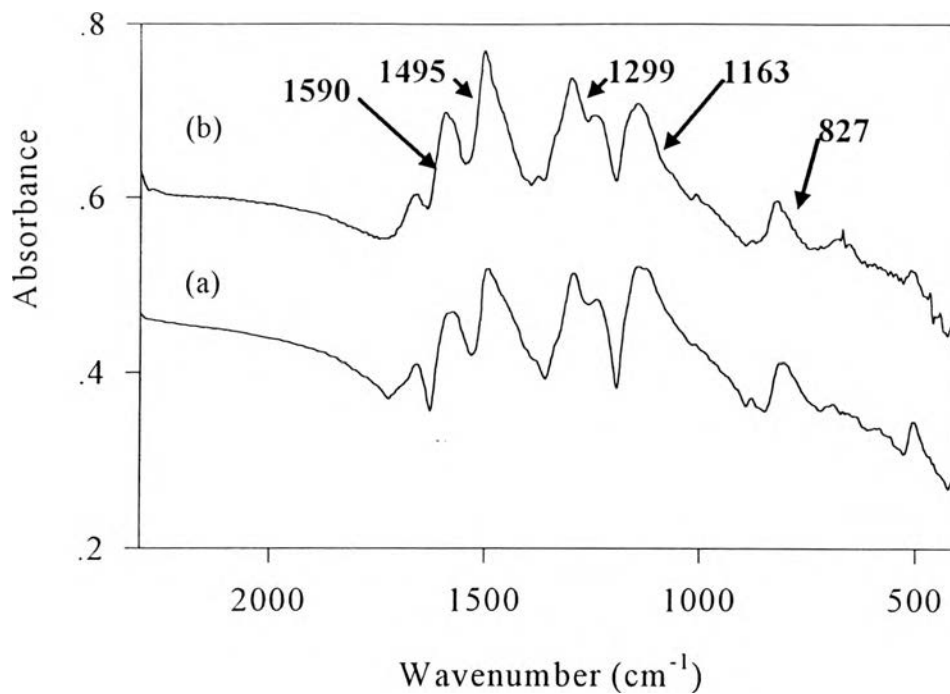


Figure 4.9 FT-IR spectra of CH₃COOH doped-polyaniline films at C_a/C_p of (a) 1:1 ($N_a/N_p=5.9E+00$) and (b) 1000:1 ($N_a/N_p=5.9E+03$).

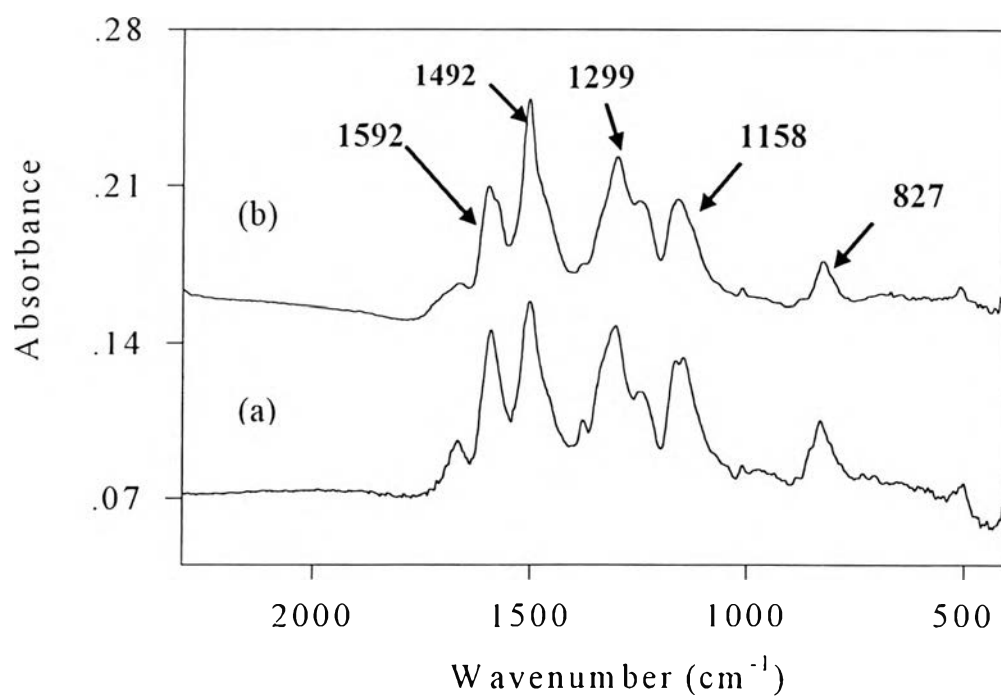


Figure 4.10 FT-IR spectra of C₅H₁₁COOH doped-polyaniline films at C_a/C_p of (a) 1:1 ($N_a/N_p=3.1E+00$) and (b) 1000:1 ($N_a/N_p=3.1E+03$).

4.1.3 Thermal Gravimetric Analysis (TGA)

TGA chromatogram of the polyaniline emeraldine base film measured in N_2 is shown in Figure 4.11. It shows a typical two-step weight loss behavior. In the first step, 1-2% weight loss at temperature up to $70^\circ C$ can be seen. This can be attributed to the loss of water molecules from the polymer film (Palamappan and Narayana, 1994). After the initial weight loss, the TGA chromatogram shows a gradual weight loss which may be assigned to the loss of low-molecular weight oligomer. It does not show a significant weight loss until $510^\circ C$, where the skeletal of polyaniline backbone began to decompose (Li and Wan, 1999).

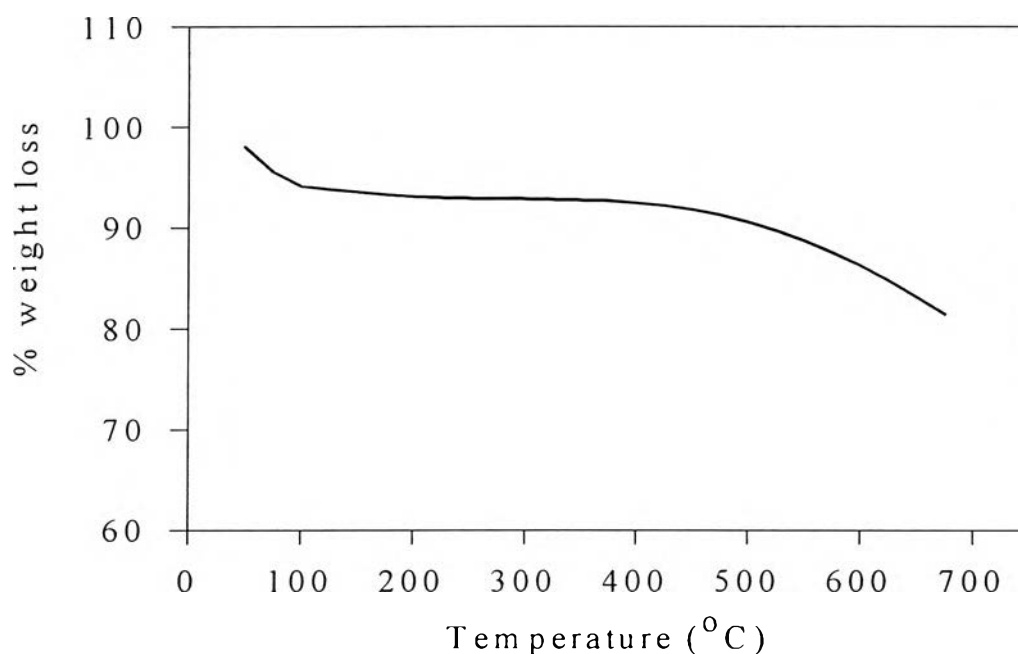


Figure 4.11 The TGA thermogram of polyaniline emeraldine base film (undoped form).

Figures 4.12-4.15 show the TGA chromatograms of polyaniline films doped with HCl , H_3PO_4 , CH_3COOH and $C_5H_{11}COOH$. After doping, the TGA thermogram of polyaniline salts shows the three-step weight loss behavior. For the first-step weight loss, TGA thermogram shows 2-20%

weight-loss at the temperature between 50 and 100°C in which, initially, water escaped from the polymer chain, followed by the loss of solvent at the temperature 200°C. The third-step weight loss corresponded to the loss of acid dopants and the decomposition of polyaniline backbone chain up to 400°C for HCl-doped polyaniline and 550°C for H₃PO₄-doped polyaniline (Pielichowski, 1997). The TGA chromatograms of polyaniline films doped with weak acids; CH₃COOH and C₅H₁₁COOH also show the three-step weight loss behavior. In the first step, there is 1-2 % weight loss at the temperature about 60-70°C due to the loss of water molecules. At temperature up to 200°C, NMP solvent was lost from the polymer film. The third-step weight loss is present at the temperature above 500°C and 450°C for CH₃COOH and C₅H₁₁COOH-doped polyanilines respectively, corresponding to the decomposition of the polymer chains.

Thermal stability of polyaniline films strongly depends on the counter ions used. Referring to Figure 4.6, the polyaniline doped with H₃PO₄ was the most stable film. It shows the highest third-step weight loss temperature, above 550°C, and still maintained 40% of its original weight after 700°C. The reasons for that may be due to the highest boiling point of H₃PO₄, and because it was inert towards oxidation and reduction (Palaniappan and Narayana, 1994). The second reason is the benzene segment in polyaniline chain can condense with H₃PO₄ to produce phosphoamide (Li and Wan, 1999), because the N-H bond is one of the weakest bonds and nitrogen atoms in benzene segment is the most reactive atom in polyaniline chain, this phosphoamide can stabilize the polyaniline chain (Li and Wan, 1999).

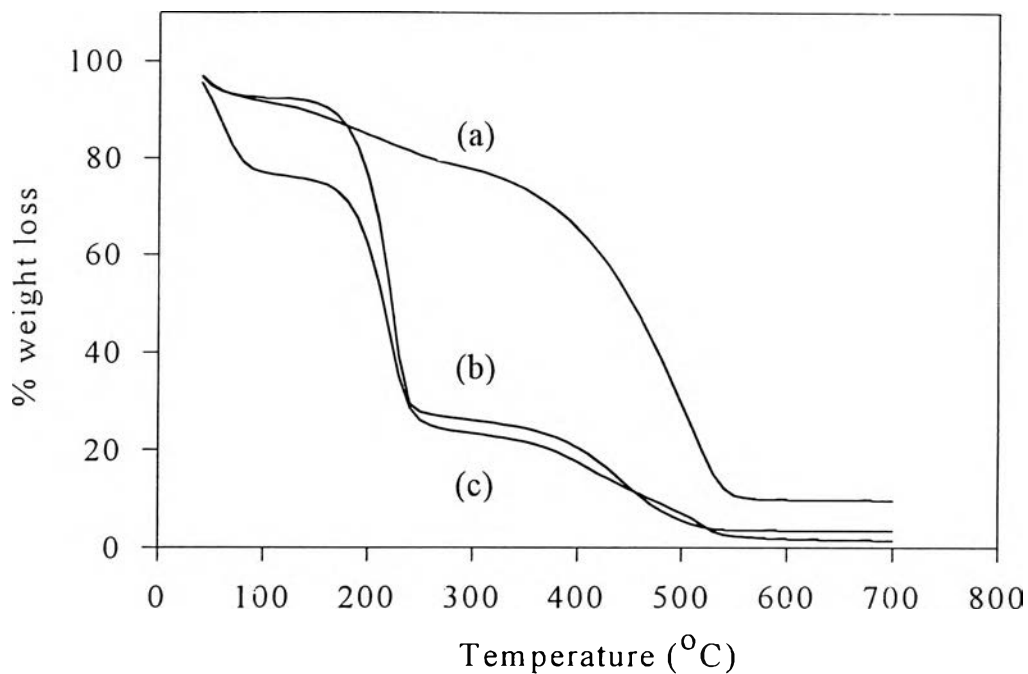


Figure 4.12 The TGA thermogram of HCl-doped polyaniline at acid/polymer concentration ratios of (a) 1:1 ($N_a/N_p=9.8E+00$), (b) 10:1 ($N_a/N_p=9.8E+01$) and (c) 100:1 ($N_a/N_p=9.8E+02$).

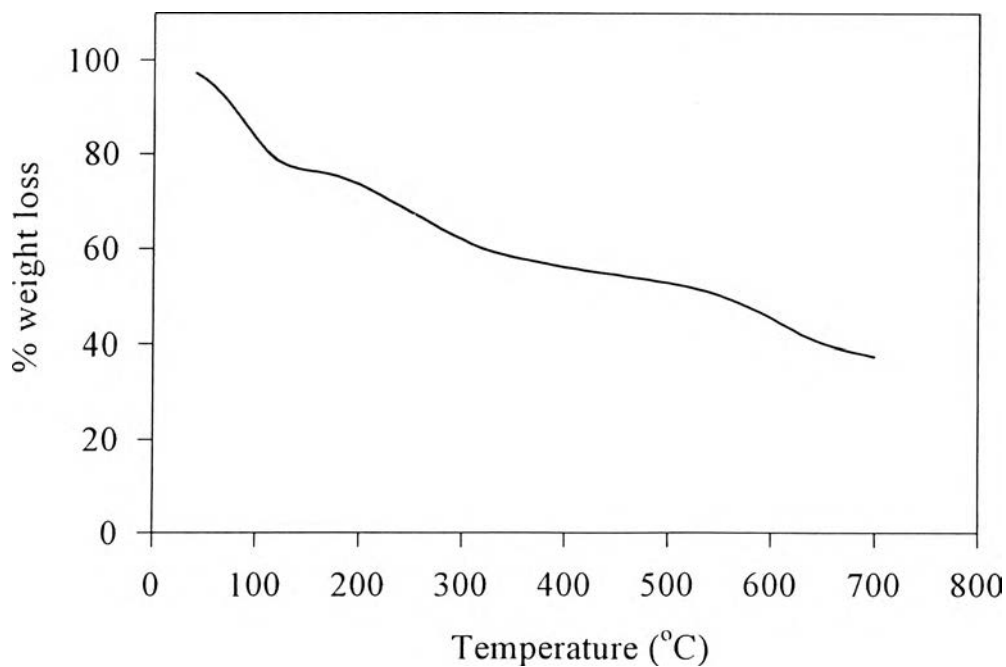


Figure 4.13 The TGA thermogram of H₃PO₄-doped polyaniline doped at acid/polymer concentration ratio of 10:1 ($N_a/N_p=3.6E+01$).

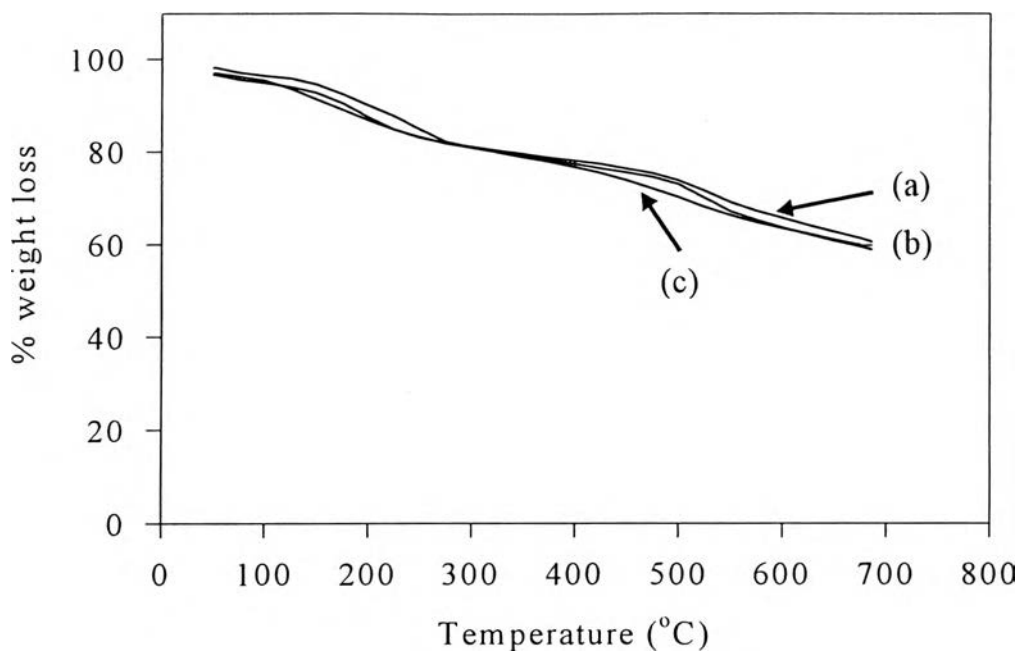


Figure 4.14 The TGA thermogram of CH₃COOH doped-polyaniline at C_a/C_p of (a) 1:1 ($N_a/N_p=5.9E+00$), (b) 100:1 ($N_a/N_p=5.9E+02$), and (c) 1000:1 ($N_a/N_p=5.9E+03$).

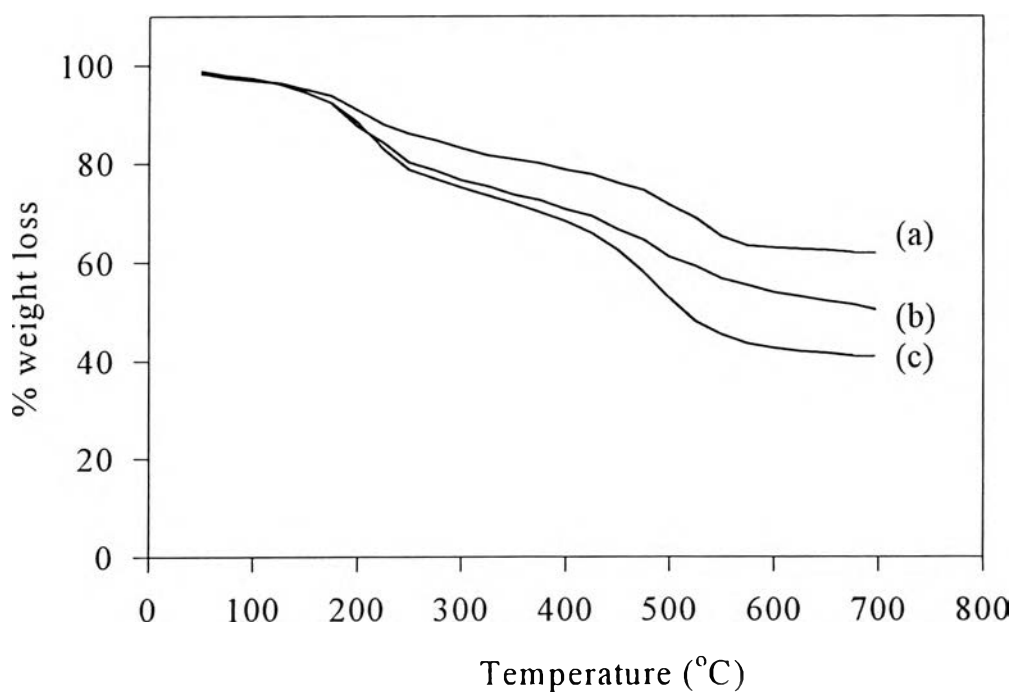


Figure 4.15 The TGA thermogram of C₅H₁₁COOH doped-polyaniline at C_a/C_p of (a) 1:1 ($N_a/N_p=3.1E+00$), (b) 100:1 ($N_a/N_p=3.1E+02$), and (c) 1000:1 ($N_a/N_p=3.1E+03$).

4.1.4 X-Ray Diffractometry (XRD)

A typical X-ray pattern of polyaniline emeraldine base is shown in Figure 4.16. Its pattern consists only of a broad band at $2\theta \sim 25^\circ$, which can be associated with X-ray diffraction of amorphous region in the sample (Pouget *et al.*, 1991).

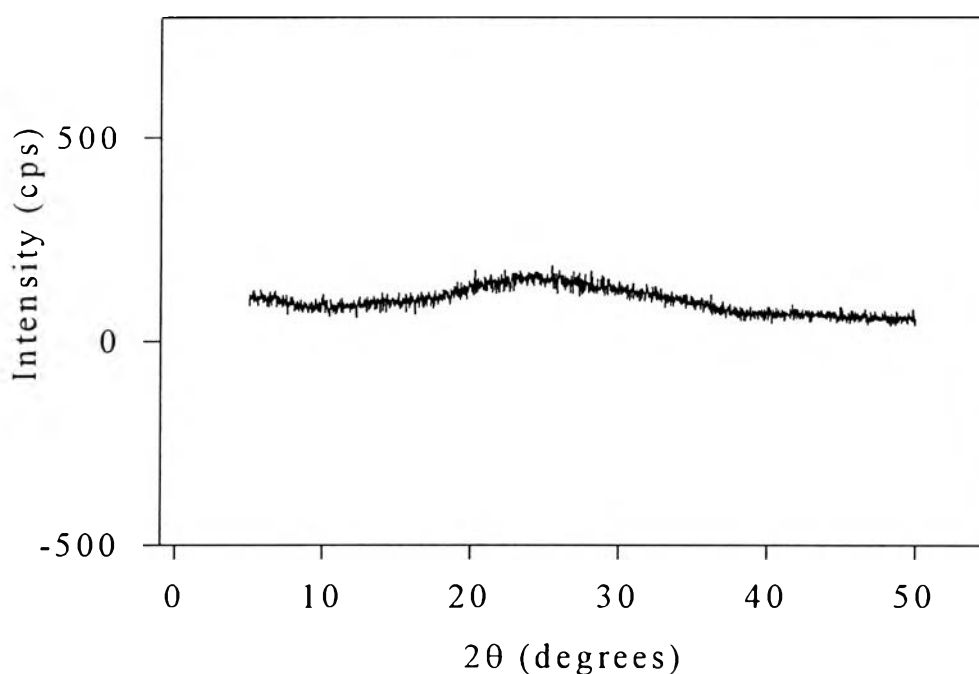


Figure 4.16 The XRD pattern of emeraldine base film.

Figure 4.17 shows the XRD pattern of polyaniline films doped with HCl at various acid/polymer concentration ratios. It is interesting to find that when acid/polymer concentration ratio was increased to 10:1, the crystalline structure was formed. More positive charges at the higher HCl concentrations induced higher doping levels. The repulsive effect of these positive charges caused the polymer chains to expand toward crystalline structures. The main characteristic peaks at $2\theta \sim 11^\circ$ (d spacing $\sim 8.04 \text{ \AA}$) indicates the distance between the polymer chains, thus it can correspond to the (001) reflection. The peak at $2\theta \sim 14^\circ$ represents the N-Cl distance in the polymer chain (Pouget *et al.*, 1991). All the main reflection observed in the

XRD pattern can be indexed in a pseudoorthorhombic cell with lattice parameters $a = 4.2 \text{ \AA}$, $b = 6.1 \text{ \AA}$ and $c = 8.0 \text{ \AA}$. When HCl concentration was further increased, the degree of crystallinity decreased and its structure became amorphous again, causing from the loss of planarity due to the steric effect of excess Cl substituted in the polymer chains.

Pouget *et al.*, (1991) showed that the polyaniline films prepared by solution casting exhibited partially crystalline structure and the insulating base form was essentially amorphous. This emeraldine base had the structure similar to that of chemically analogous polymers such as poly(phenylene sulfide) and poly(phenylene oxide).

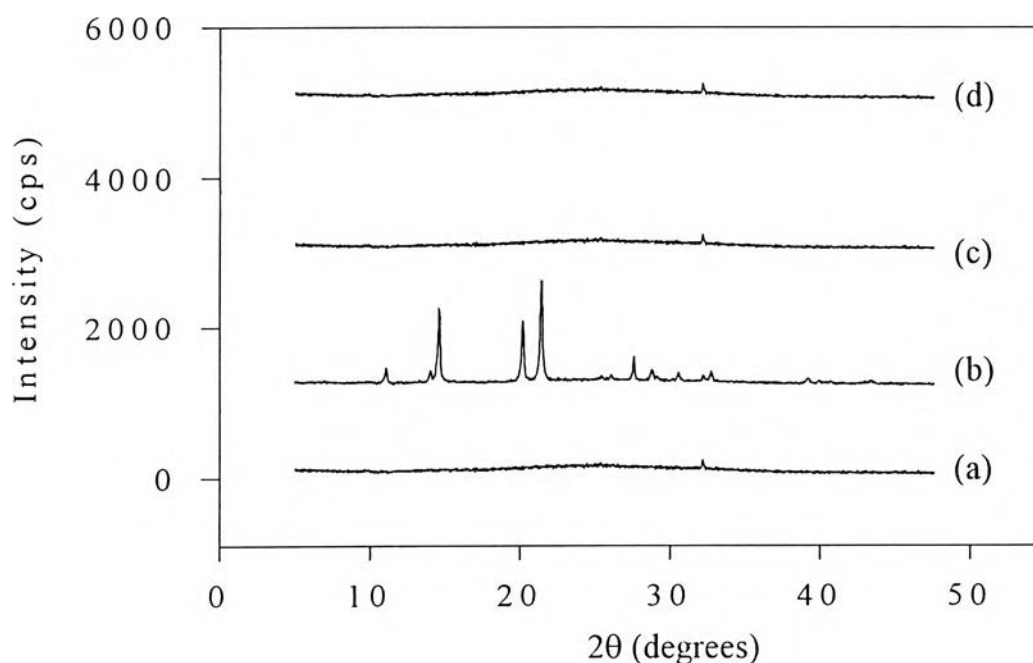


Figure 4.17 The XRD pattern of HCl-doped polyaniline films at C_a/C_p of (a) 1:1 ($N_a/N_p=9.8E+00$), (b) 10:1 ($N_a/N_p=9.8E+01$), (c) 100:1 ($N_a/N_p=9.8E+02$) and (d) 1000:1 ($N_a/N_p=9.8E+03$).

Table 4.5 The assignment of XRD pattern of HCl-doped polyaniline films at $C_a/C_p = 10:1$ (Pouget *et al.*, 1991)

2θ (deg.)	d-spacing, (\AA°) (experiment)	d-spacing, (\AA°) (reference)	$(hkl)^*$	Assignments
11.0	8.04	9.57	(001)	Distance between polymer chains
14.6	6.07	5.94	(010)	Cl-N distance
21.4	4.15	4.26	(100)	-
26.0	3.42	3.51	{{(110)}}	-
27.5	3.24	3.28	{{(111)}}	-
28.8	3.09	2.98	(020)	-
30.5	2.93	2.85	{{(112)}}, {{(021)}}	-
32.66	2.73	2.47	{{(120)}}	-
39.14	2.29	2.34	{{(121)}}, {{(113)}}	-

* (hkl) means the Miller indices of planes

{{ (hkl) }} means a set of reflections with permutation of the sign of the Miller indices

Figures 4.18-4.20 show the XRD patterns of polyaniline films doped with H_3PO_4 , CH_3COOH and $\text{C}_5\text{H}_{11}\text{COOH}$, respectively. Their patterns show the amorphous structure similar to that of emeraldine base at all acid/polymer concentration ratios because these acids have lower efficiency to protonate H^+ to the polymer chains compared to polyaniline doped with HCl.

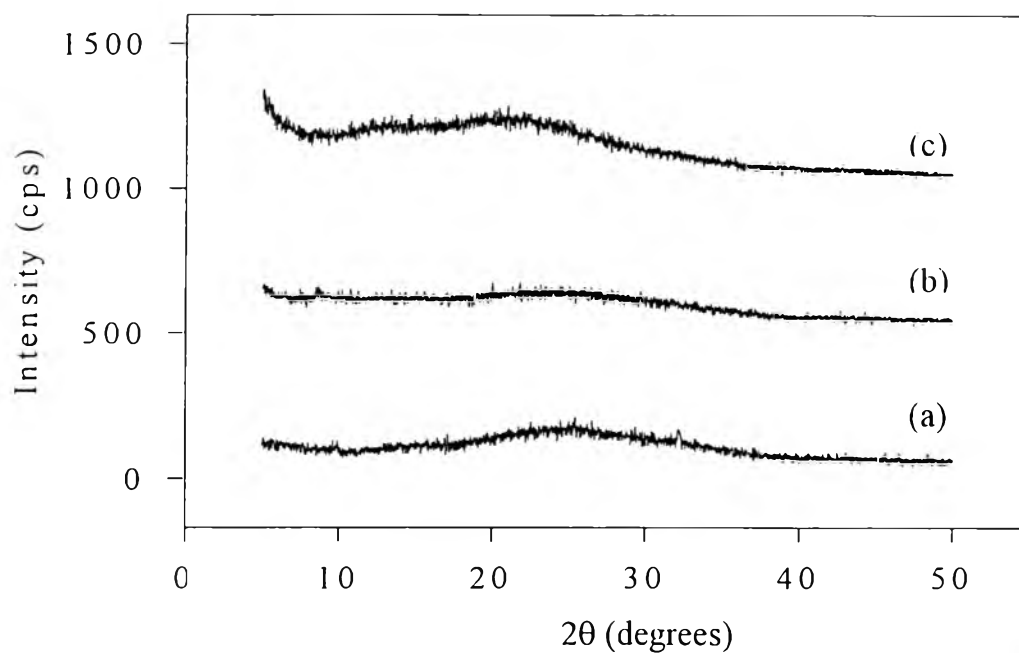


Figure 4.18 The XRD patterns of H_3PO_4 -doped polyaniline films at C_a/C_p of (a) 1:10 ($N_a/N_p=3.6\text{E}-01$), (b) 1:1 ($N_a/N_p=3.6\text{E}+00$), and (c) 1:1 ($N_a/N_p=3.6\text{E}+01$).

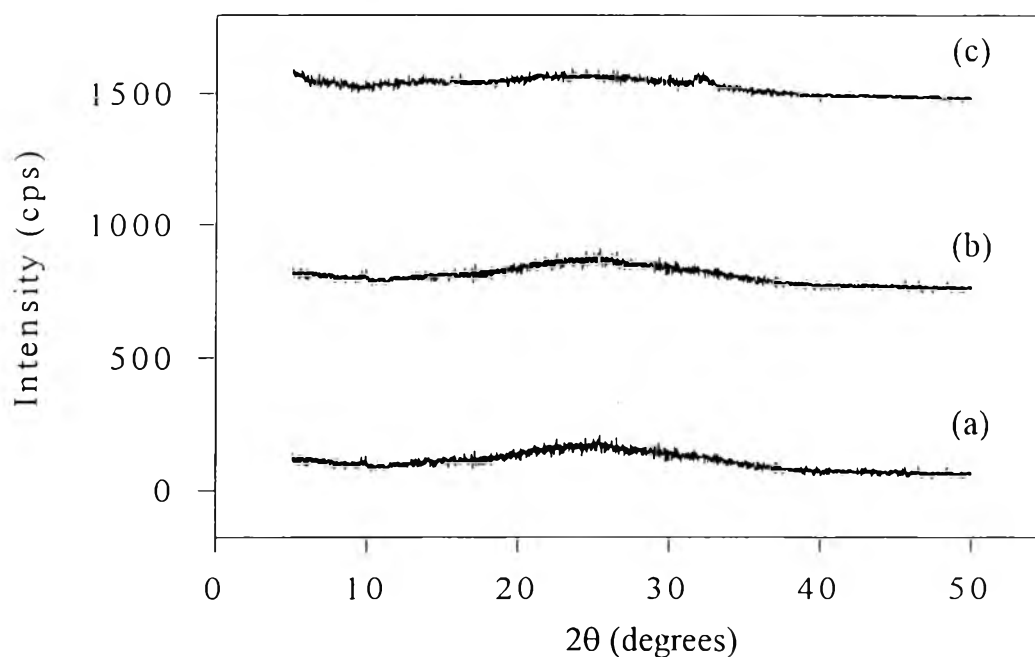


Figure 4.19 The XRD patterns of CH_3COOH -doped polyaniline films at C_a/C_p of (a) 1:1 ($N_a/N_p=5.9\text{E}+00$), (b) 100:1 ($N_a/N_p=5.9\text{E}+02$), and (c) 5000:1 ($N_a/N_p=2.9\text{E}+04$).

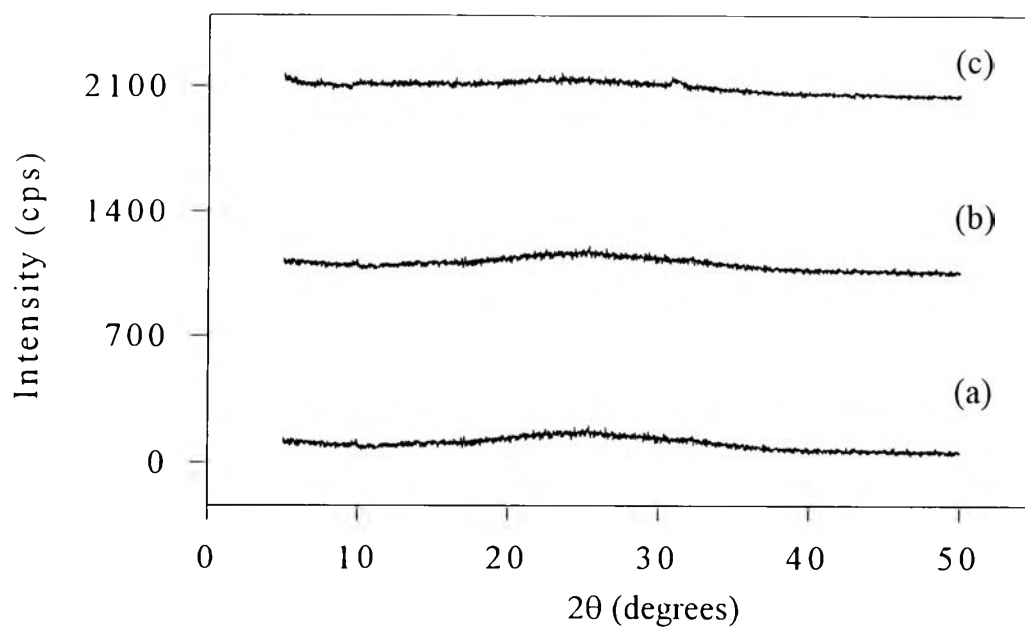


Figure 4.20 The XRD patterns of $C_5H_{11}COOH$ -doped polyaniline films at C_a/C_p of (a) 1:1 ($N_a/N_p=3.1E+00$), (b) 100:1 ($N_a/N_p=3.1E+02$), and (c) 5000:1 ($N_a/N_p=1.5E+04$).

4.1.5 Scanning Electron Microscope (SEM)

SEM was used to study the morphology of polyaniline films after doping with different acid dopant types and acid/polymer concentration ratios because the morphology of polyaniline can be influenced by these two parameters.

SEM micrographs (magnification 5000 times) of polyaniline films doped with HCl and H₃PO₄ are shown in Figure 4.21 and Figure 4.22. It was found that the network structures were formed when acid/polymer concentration ratios increased due to the formation of H-bonding between the polymer chains. In the case of HCl doped polyaniline film, at very high acid/polymer concentration ratios ($C_a/C_p=1000:1$), the surface of film became smooth resulting from the loss of crystallinity of the polymer films due to the steric effect of excess Cl⁻ substituted on benzene rings as mentioned in XRD pattern shown in Figure 4.17. When polyaniline films were doped with CH₃COOH and C₅H₁₁COOH, the morphology of these polyaniline films showed the smooth surface both at low and very high acid/polymer concentration ratios because these two acids have much lower efficiency to protonate H⁺ to polymer chains compared to HCl and H₃PO₄. A less amount of hydrogen, a less amount of H-bonding and a smooth surface was formed.

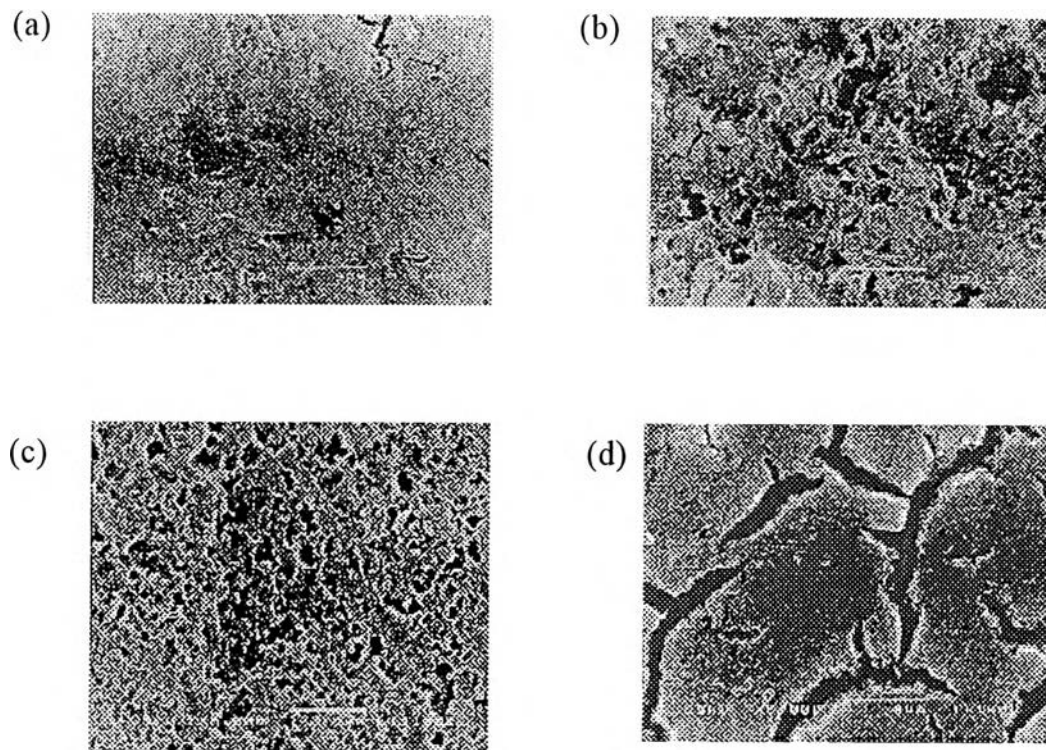


Figure 4.21 The SEM micrographs of HCl-doped polyaniline films at C_a/C_p of (a) 1:1 ($N_a/N_p=9.8E+00$), (b) 10:1 ($N_a/N_p=9.8E+01$), (c) 100:1 ($N_a/N_p=9.8E+02$), and (d) 1000:1 ($N_a/N_p=9.8E+03$) with magnification of 5000:1.

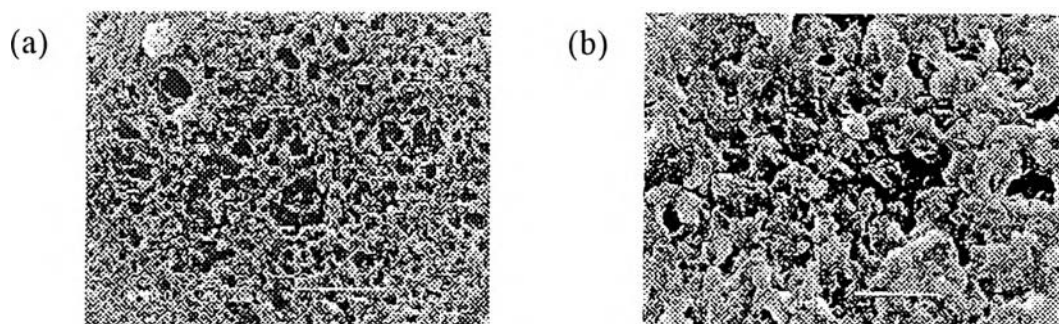


Figure 4.22 The SEM micrographs of H₃PO₄-doped polyaniline films at C_a/C_p of (a) 1:10 ($N_a/N_p=3.6E-01$), (b) 1:1 ($N_a/N_p=3.6E+00$) and (c) 10:1 ($N_a/N_p=3.6E+01$) with magnification of 5000:1.

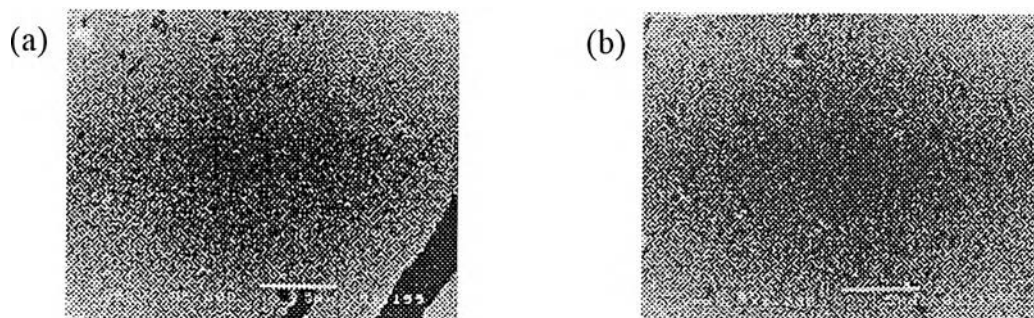


Figure 4.23 The SEM Micrographs of CH_3COOH -doped polyaniline films at C_a/C_p of (a) 1:1 ($N_a/N_p=5.9\text{E}+00$) and (b) 1000:1 ($N_a/N_p=5.9\text{E}+03$) with magnification of 5000:1.

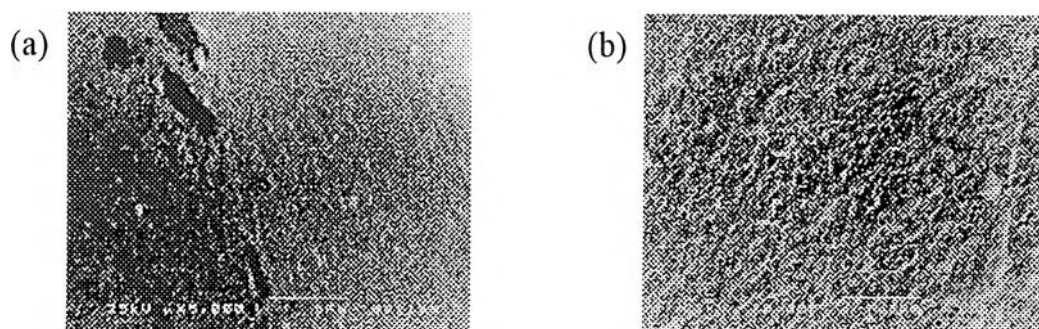


Figure 4.24 The SEM micrographs of $\text{C}_5\text{H}_{11}\text{COOH}$ -doped polyaniline films at C_a/C_p of (a) 1:1 ($N_a/N_p=3.1\text{E}+00$) and (b) 1000:1 ($N_a/N_p=3.1\text{E}+03$) with magnification of 5000:1.

Huang *et al.*, (1986) reported that the SEM micrographs of emeraldine hydrofluoroborate film grown electrochemically on a platinum anode showed a compact microspheroid surface morphology. The emeraldine hydroperchlorate film grew electrochemically on an indium oxide conducting glass showed the fibrillar structure. It was not known whether the difference in morphology between these two emeraldine salt samples was due to the different anions employed the nature of the electrode or the difference in the electrochemical procedures used.

4.2 Electrical Conductivity

4.2.1 Effect of Aging Time on the Specific Conductivity

To study the effect of aging time on the specific conductivity, the doped polyaniline films were stored in the dessicator before the measurement by the four-point probe meter at 25°C. Figure 4.25 shows the specific conductivity of the HCl-doped polyaniline films. The specific conductivity decreased with aging time and attained equilibrium states after 20 days. This resulted from the evaporation of moisture in the polymer films. As seen in Figure 4.26, the amount of moisture content decreased with the number of days stored and it seemed to reach constant values after 20 days. These two plots indicated that the amount of moisture content had a direct effect on the specific conductivity. The effect of moisture contents will be further discussed in section 4.2.3.

Compared with the HCl-doped polyaniline films, the specific conductivities of the polyaniline films doped with CH_3COOH and $\text{C}_5\text{H}_{11}\text{COOH}$ remained unchanged after aging, indicating that the amount of moisture content had little affect on the specific conductivity, relative to the HCl-doped polyaniline as shown in Figures 4.27-4.28.

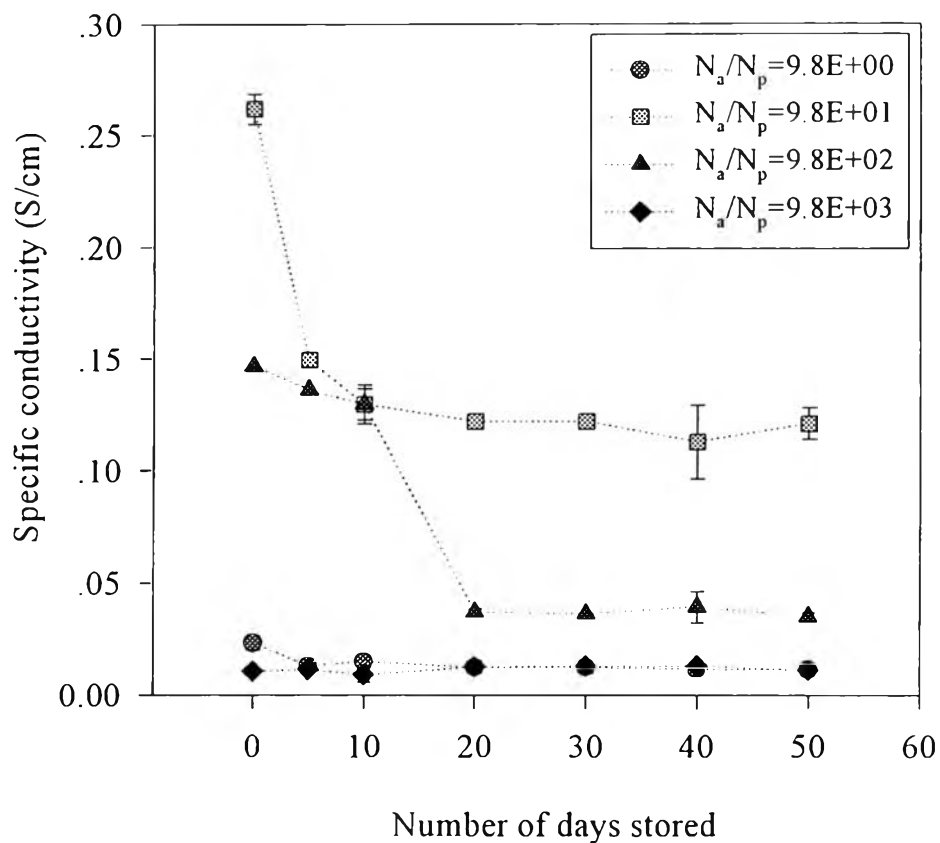


Figure 4.25 The specific conductivity of HCl-doped polyaniline films *versus* numbers of days stored at 25°C, with relative humidity between 65-70%.

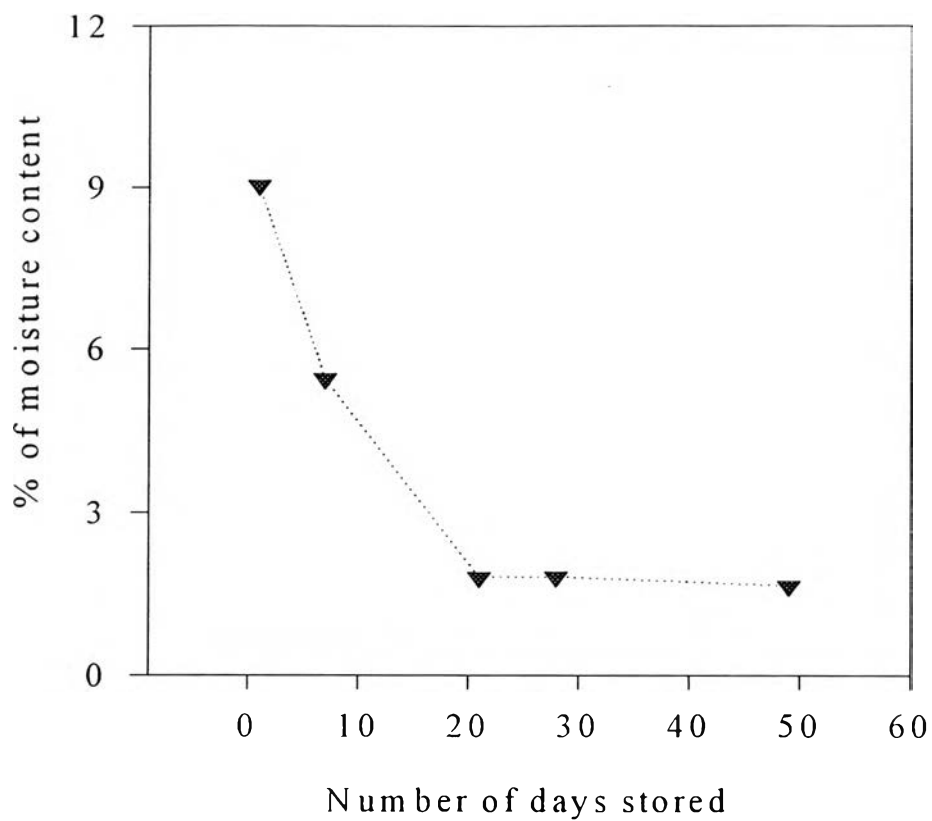


Figure 4.26 The relationship between amount of moisture and number of days stored of HCl-doped polyaniline at $C_a/C_p=10:1$ ($N_a/N_p=9.8E+01$) at 25°C , with relative humidity between 65-70%.

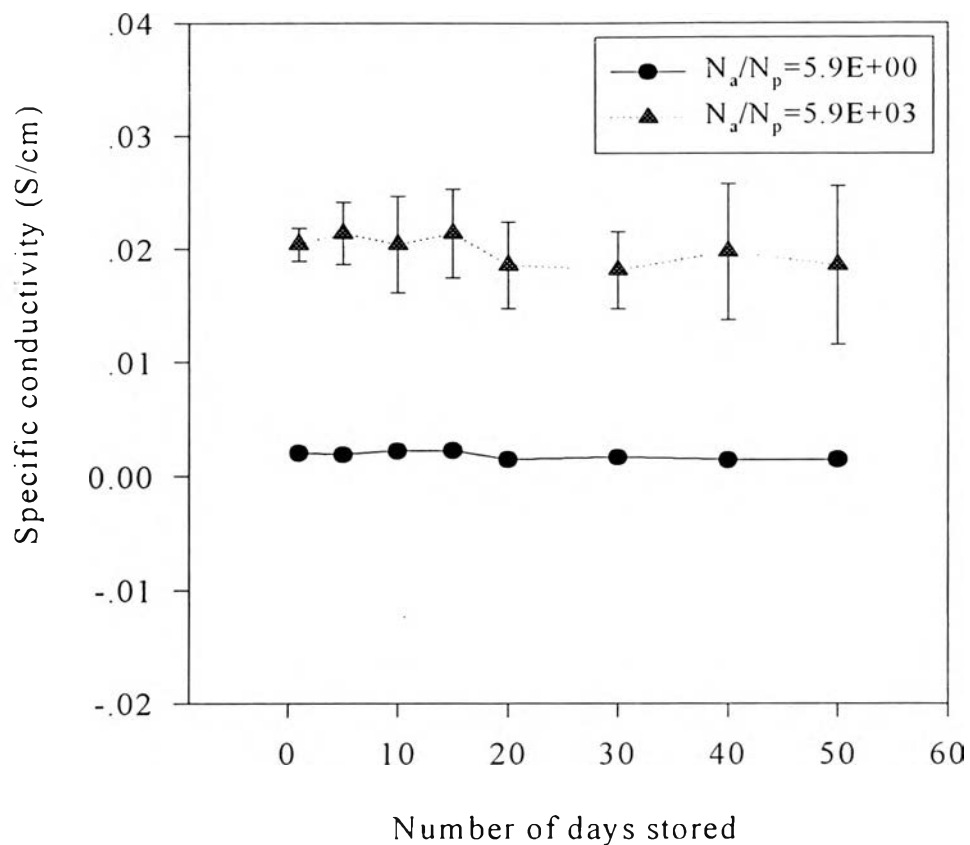


Figure 4.27 The specific conductivity of CH_3COOH -doped polyaniline films *versus* number of days stored at 25°C , with relative humidity between 65-70%.

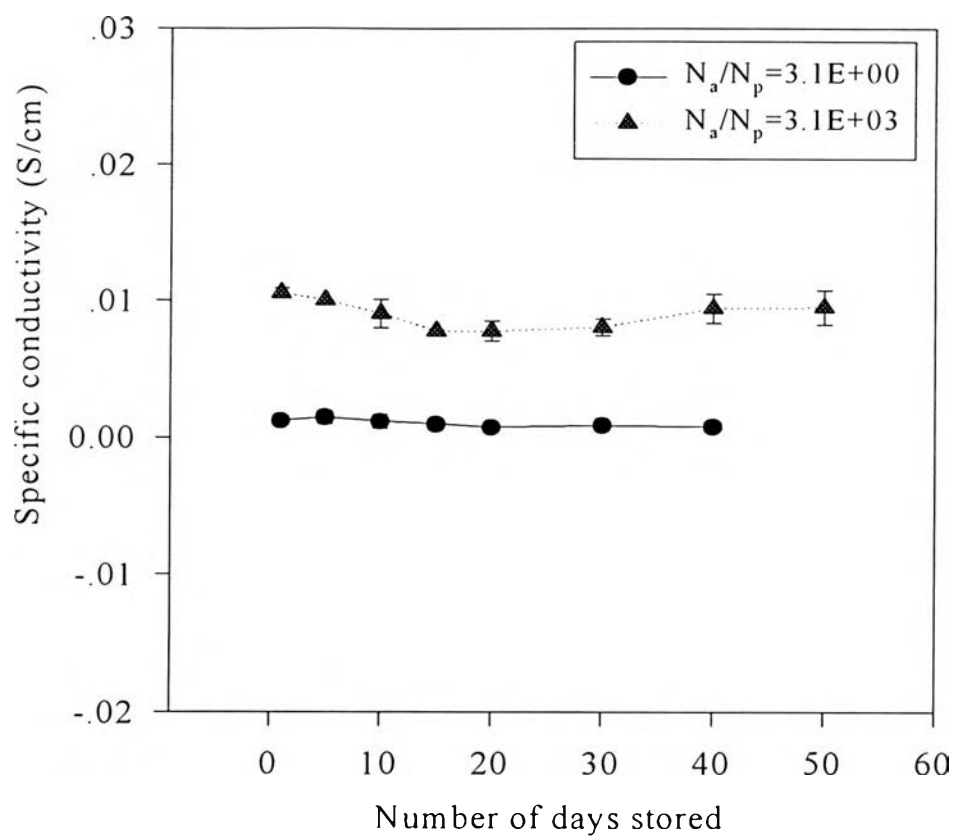


Figure 4.28 The specific conductivity of $C_5H_{11}COOH$ -doped polyaniline films *versus* number of days stored at $25^\circ C$, with relative humidity between 65-70 %.

4.2.2 Effect of Dopant Types and Acid/Polymer Concentration Ratios (C_a/C_p) on the Specific Conductivity

In this work, HCl, H_3PO_4 , CH_3COOH and $C_5H_{11}COOH$ were used as acid dopants. The conductivity of the doped polyaniline films was measured by using the four-point probe meter at $25^\circ C$.

For the HCl-doped polyaniline, the specific conductivity increased with C_a/C_p . The highest specific conductivity occurred at $C_a/C_p=10:1$ ($N_a/N_p=9.8E+01$), and beyond that the specific conductivity decreased as shown in Figure 4.29. This result can be supported by FT-IR and XRD data which showed the highest degree of crystallinity at $C_a/C_p=10:1$ ($N_a/N_p=9.8E+01$) as shown in Figure 4.16. For further increase in C_a/C_p , the degree of crystallinity decreased due to the steric effect of Cl^- substituent on the polymer chain resulting in a decrease in the electronic conjugation length (Morales *et al.*, 1997).

For the CH_3COOH and $C_5H_{11}COOH$ -doped polyanilines, the specific conductivity increased gradually with C_a/C_p and attained equilibrium at about $C_a/C_p=1000:1$ ($N_{AcOH}/N_p=5.9E+03$, $N_{Hex}/N_p=3.1E+03$). The increase in conductivity occurred due to an increase in the degree of protonation on the polyaniline chains; more positive charges were produced and the electronic conjugation length was increased. Beyond $C_a/C_p>1000:1$ ($N_{AcOH}/N_p=5.9E+03$, $N_{Hex}/N_p=3.01E+03$) the specific conductivity seemed to reach the constant values because the doping was complete.

In comparison with HCl, both CH_3COOH and $C_5H_{11}COOH$ were weak acids, so they had a much less efficiency to protonate H^+ to the polymer chains leading to lowering in the specific conductivity.

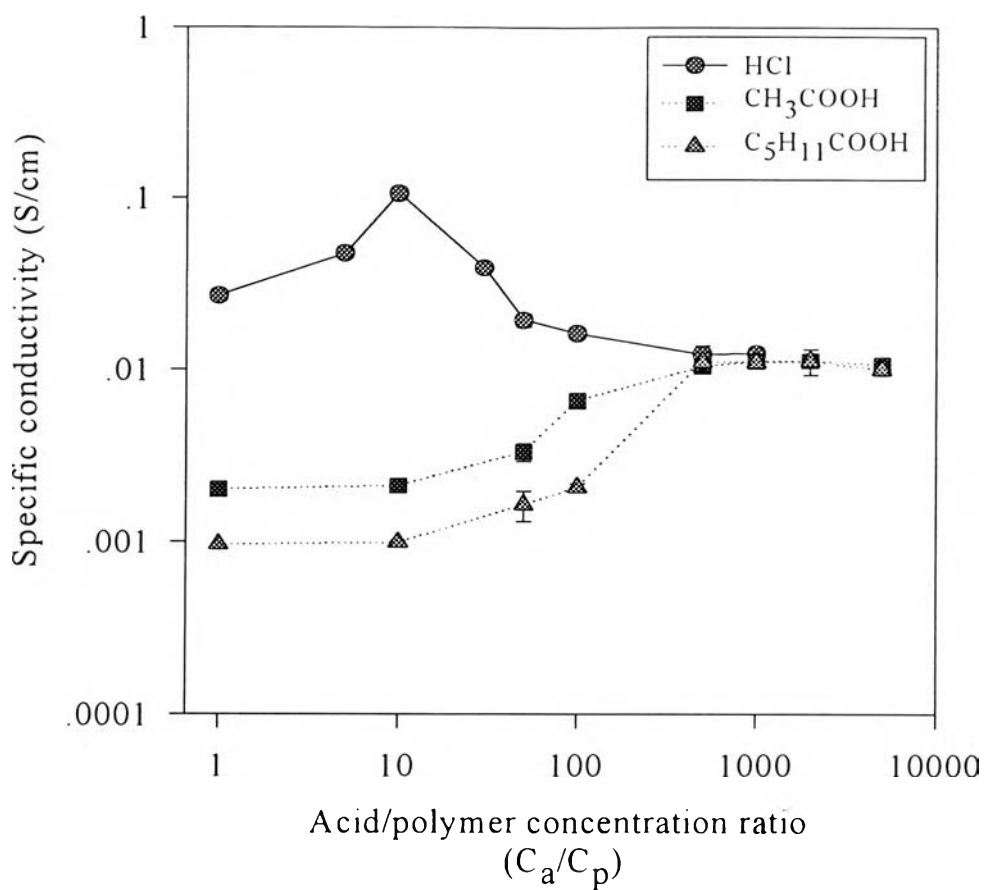


Figure 4.29 Effect of acid/polymer concentration ratios (C_a/C_p) on the specific conductivity of doped polyaniline films with HCl, CH₃COOH and C₅H₁₁COOH at 25°C, with relative humidity between 65-70%.

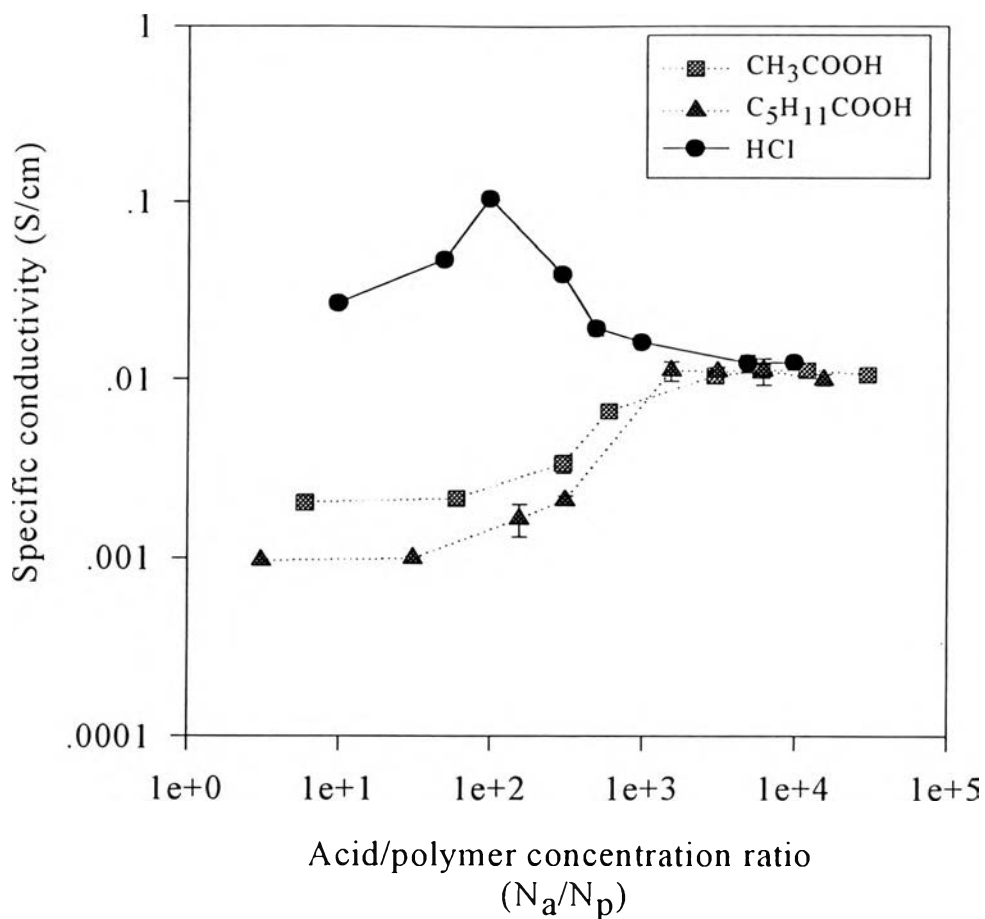


Figure 4.30 Effect of acid/polymer concentration ratios (N_a/N_p) on the specific conductivity of doped polyaniline films with HCl, CH_3COOH and $C_5H_{11}COOH$ at 25°C, with relative humidity between 65-70%.

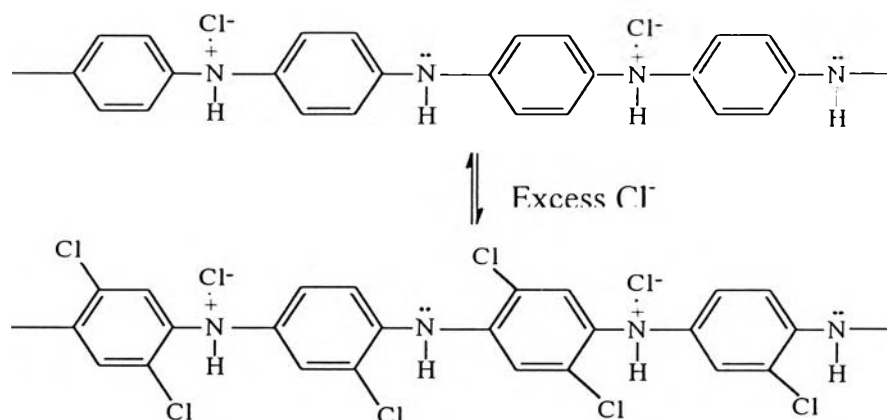


Figure 4.31 The chemical structures of polyaniline doped with an excess amount of HCl at $C_a/C_p > 10:1$ ($N_a/N_p = 98$) at 25°C, with relative humidity 65-70%.

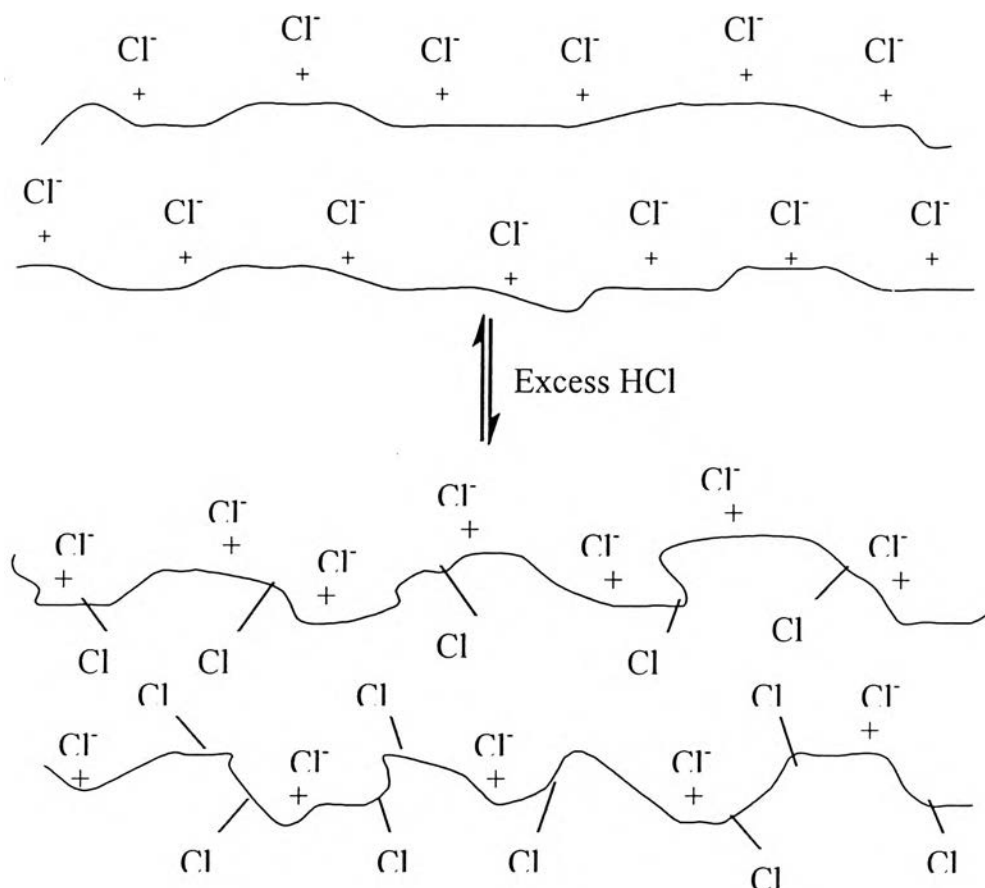


Figure 4.32 The proposed model of polyaniline doped with an excess amount of HCl concentration.

4.2.3 The Specific Conductivity of Polyaniline Films when exposed to water at 25°C

The specific conductivity of polyaniline films was observed by the four-point probe meter at 25°C. Figure 4.33 shows the specific conductivity of the HCl-doped polyaniline films before and after exposing to water at various acid/polymer concentration ratios. The graph shows an increase in the specific conductivity when exposed to water. The increase in specific conductivity was due to the increase in interchain H-transfer (MacDiarmid and Epstein, 1989); water molecule acted as a carrier to transfer H^+ from a polymer chain to another as shown in Figure 4.34. Some quinoid segments were protonated resulting in an increase in positive charges on the polymer chain and therefore electrons can delocalize along the chain more effectively. From Equation 1.7, the specific conductivity (σ) is proportional to the charge mobility (μ). When protons (H^+) were transferred, the mobility of charges increased, and hence the increase in the specific conductivity. At C_a/C_p greater than 10:1 ($N_a/N_p > 9.8E+01$), the specific conductivity decreased resulting from the over-doping as mentioned in section 4.2.2. Water molecules interacted with polymer chains with more difficulty leading to the decreases in charge mobility and specific conductivity.

Figures 4.35-4.37 show the specific conductivity of the H_3PO_4 , CH_3COOH and $C_5H_{11}COOH$ -doped polyaniline films at various C_a/C_p . They exhibited higher specific conductivity when exposed to water. This can be described by the increase in charge mobility. The specific conductivity of CH_3COOH and $C_5H_{11}COOH$ -doped polyanilines attained the equilibrium value after $C_a/C_p = 1000:1$ ($N_{AcOH}/N_p = 5.9E+03$, $N_{Hex}/N_p = 3.1E+03$) due to complete doping.

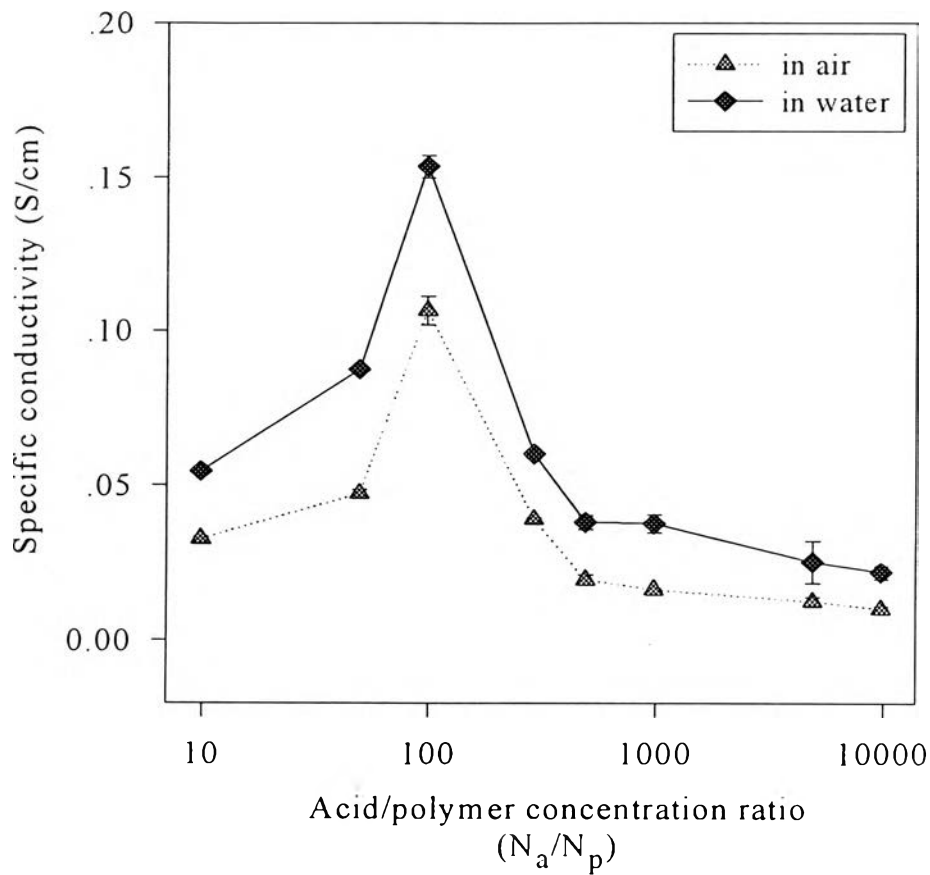


Figure 4.33 The specific conductivity of HCl-doped polyaniline films measured in air and water at various acid/polymer concentration ratios (N_a/N_p) at 25°C, with relative humidity between 65-70%.

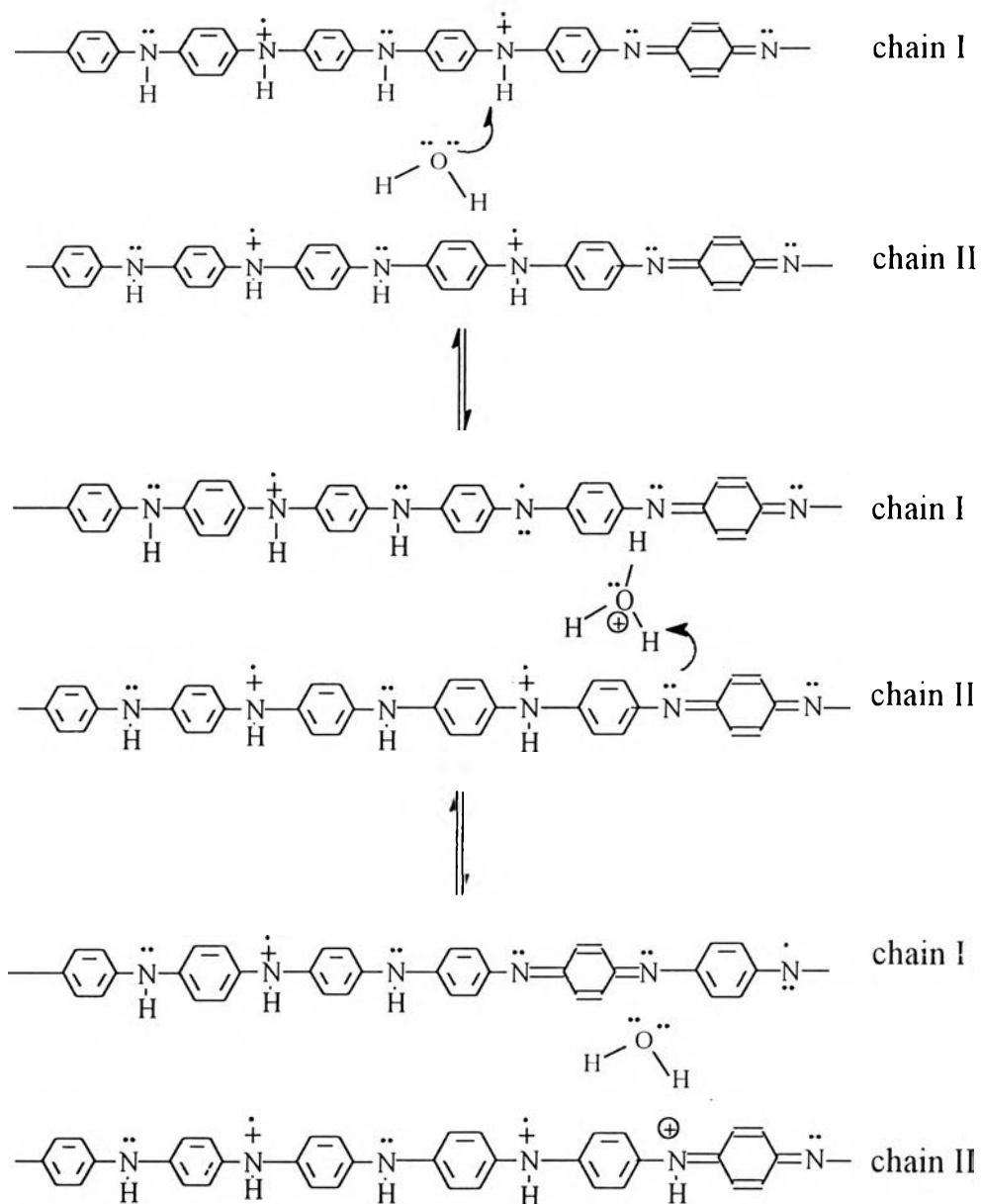


Figure 4.34 The proposed mechanism of interchain H-transfer when polymer films were exposed to water.

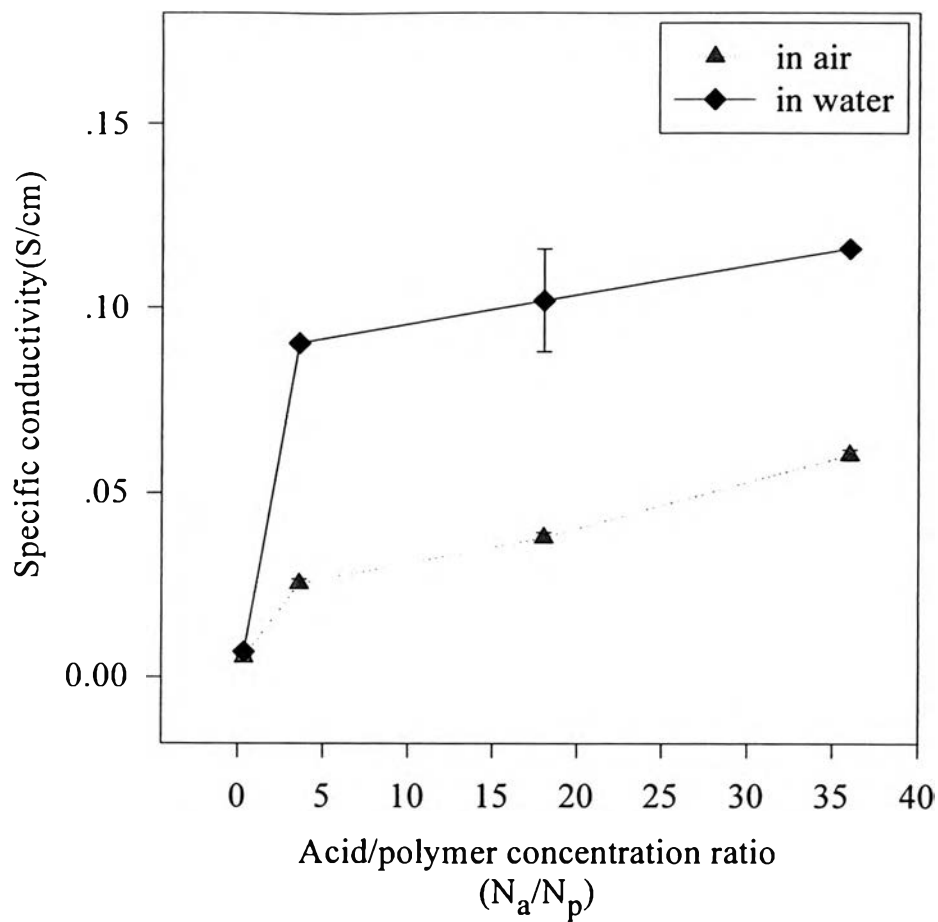


Figure 4.35 The specific conductivity of H_3PO_4 -doped polyaniline films measured in air and water at various acid/polymer concentration ratios (N_a/N_p) at 25°C, with relative humidity 65-70%.

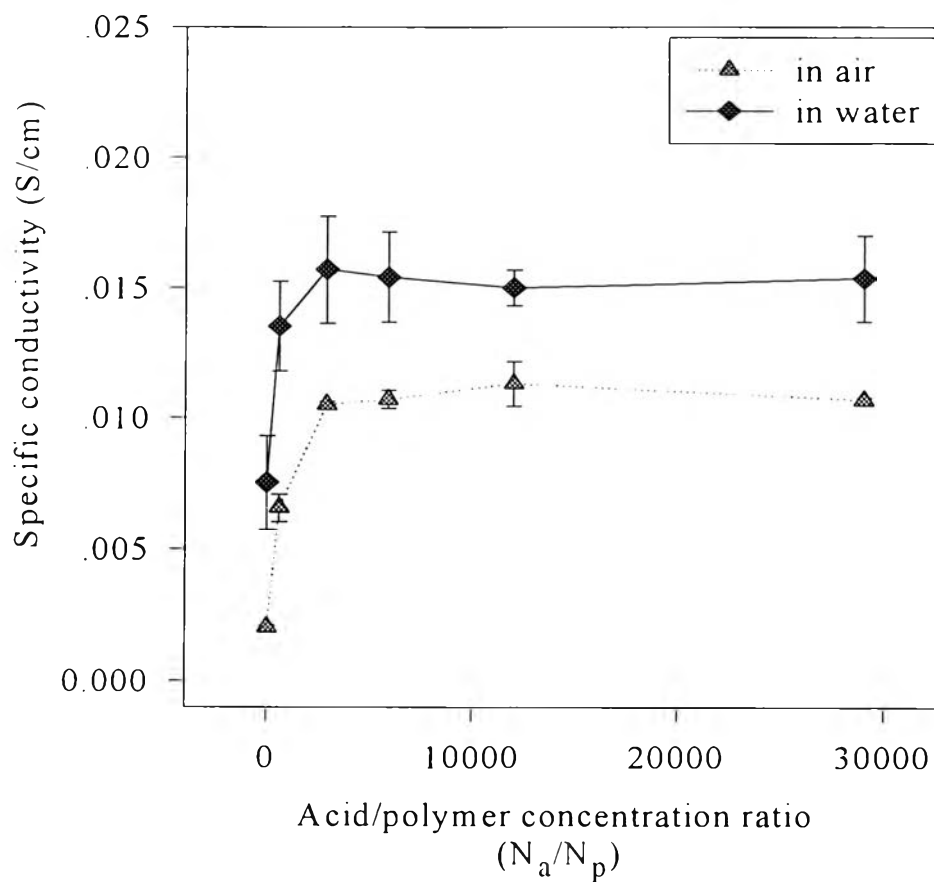


Figure 4.36 The specific conductivity of CH_3COOH -doped polyaniline films measured in air and water at 25°C , with relative humidity between 65-70%.

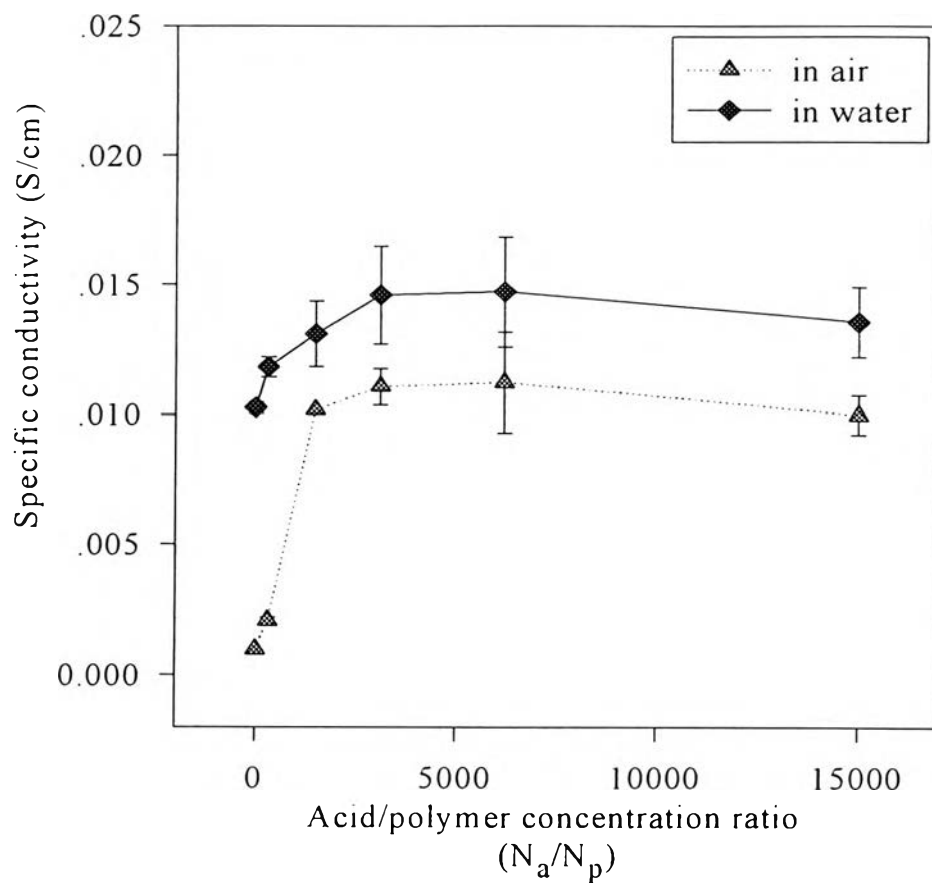


Figure 4.37 The specific conductivity of $C_5H_{11}COOH$ -doped polyaniline films measured in air and water at $25^\circ C$, with relative humidity 65-70%.

4.2.4 The Specific Conductivity of Polyaniline Films when exposed to 100% ethanol

Figure 4.38 illustrates the specific conductivity of the HCl-doped polyaniline films when exposed to 100% ethanol. The increase in the specific conductivity when exposed to 100% ethanol was also due to an increase in charge mobility and interchain H-transfer. At $C_a/C_p=10:1$ ($N_a/N_p=9.8E+01$), it shows the highest specific conductivity due to the formation of crystallinity, as shown in the XRD results. Beyond that C_a/C_p , the specific conductivity tended to decrease resulting from the loss of planarity as can be seen in Figure 4.32, and the decrease in the electronic conjugation length (MacDiarmid and Epstein, 1989).

Comparing with the polymer films when exposed to water, the polyaniline films exposed to 100% ethanol showed lower specific conductivity. This can be explained by the difference in the sizes of water and ethanol. The structure of ethanol was larger than that of water leading to a lower efficiency to transfer H^+ from polymer chains.

When the CH_3COOH -doped polyaniline films were exposed to 100% ethanol, higher specific conductivity was obtained as shown in Figure 4.39. But the values were lower compared with those of the polyaniline films exposed to water. The lower specific conductivity can be explained by the difference in the sizes of water and ethanol. The structure of ethanol was larger than that of water leading to a lower efficiency to transfer H^+ from polymer chains.

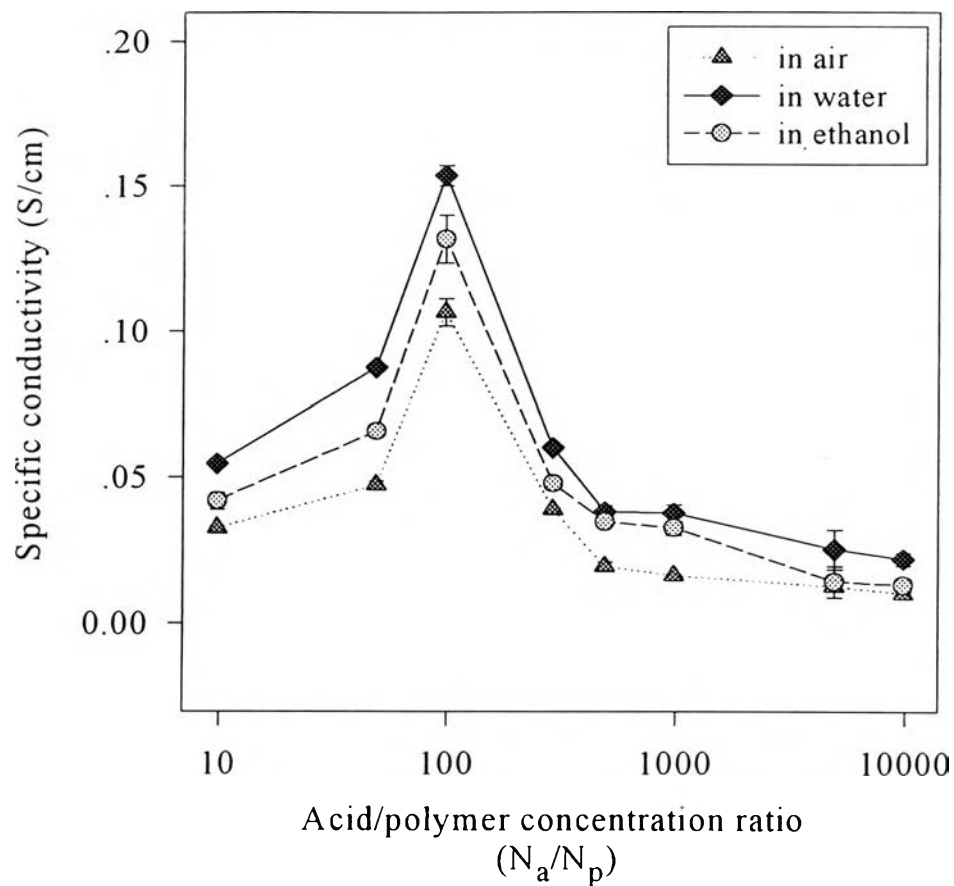


Figure 4.38 The specific conductivity of HCl-doped polyaniline films when exposed to water and 100% ethanol at 25°C, with relative humidity between 65-70%.

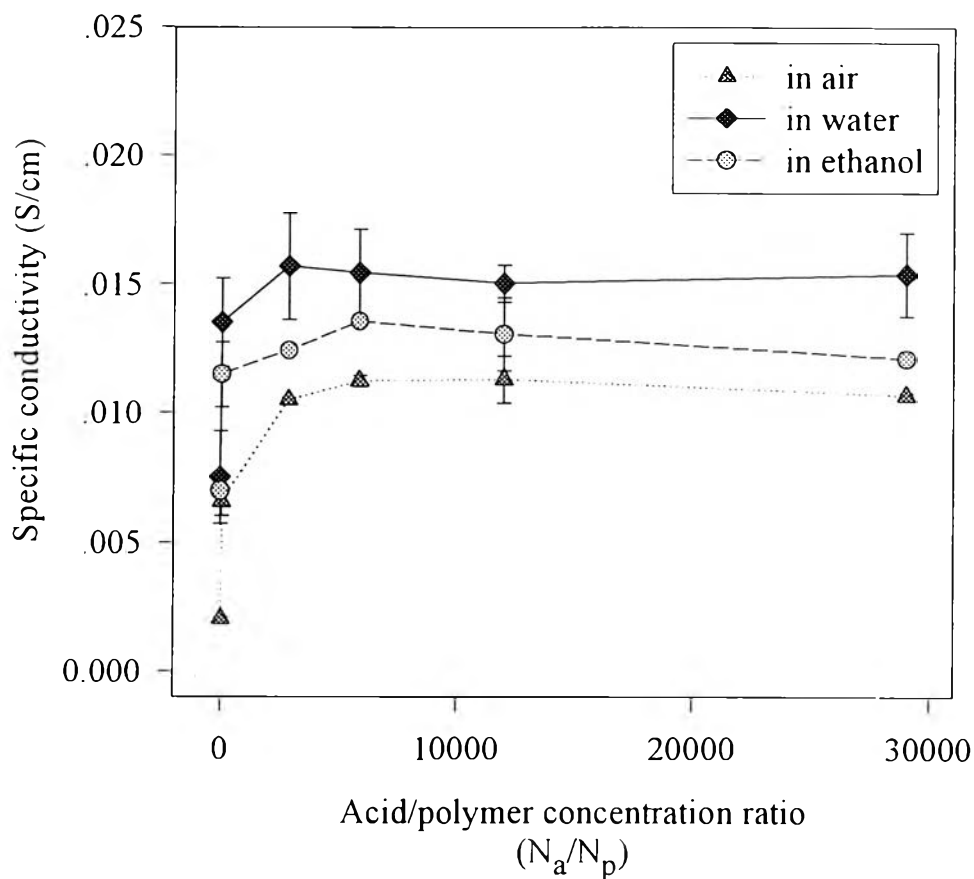


Figure 4.39 The specific conductivity of CH_3COOH -doped polyaniline films when exposed to water and 100% ethanol at 25°C , with relative humidity 65-70%.

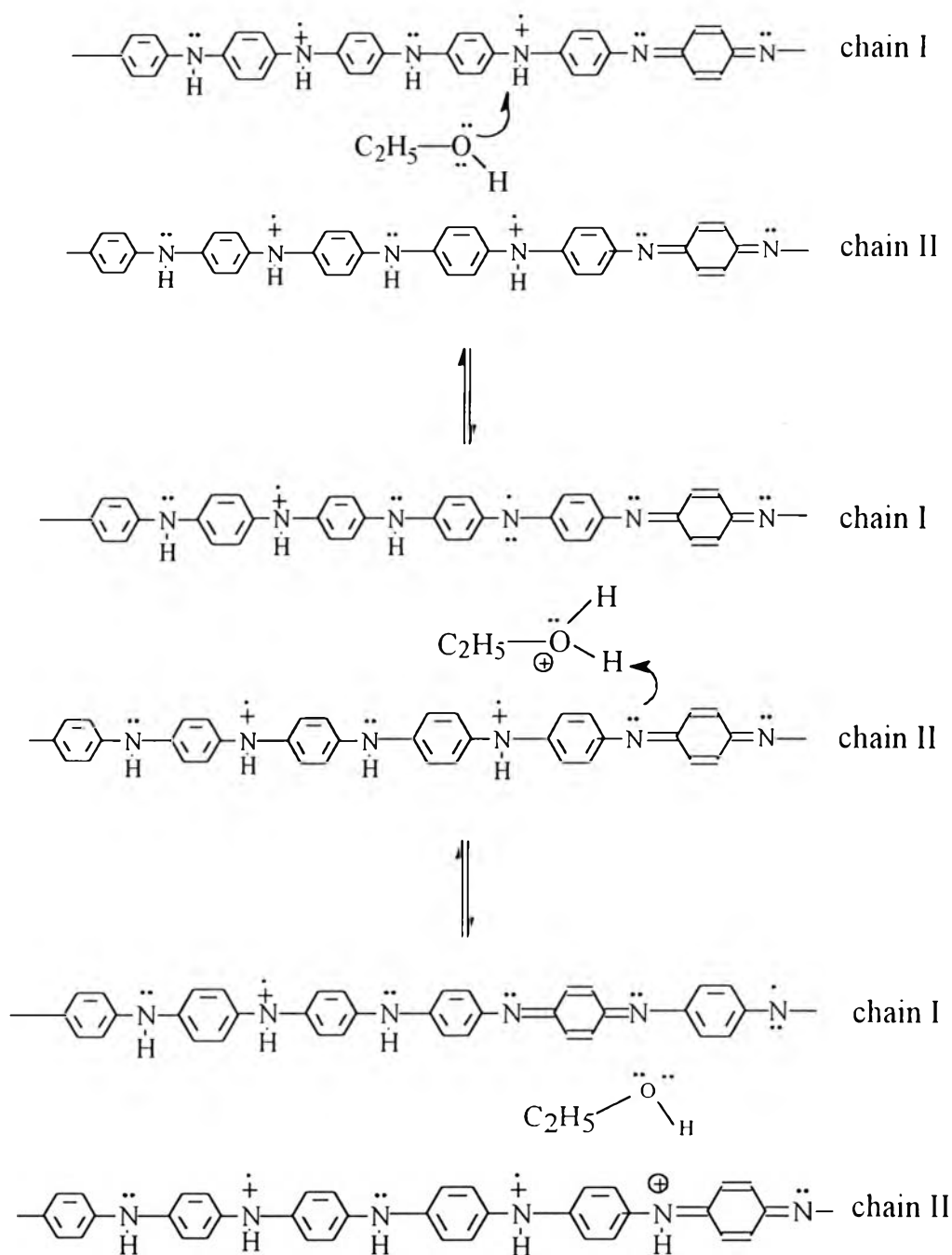


Figure 4.40 The proposed mechanism of interchain H-transfer when polyaniline film was exposed to 100% ethanol.

4.2.5 Effect of Ethanol Concentration

The effect of ethanol concentration on HCl and CH₃COOH-doped polyaniline films are shown in Figures 4.41 and 4.42, respectively. For the HCl-doped polyaniline, the specific conductivity starts to decrease at the ethanol concentration of 1.7 M and attains the saturated specific conductivity at the ethanol concentration of 8.3 M. In the case of CH₃COOH-doped polyaniline, the specific conductivity decreases at the ethanol concentration of 2.8 M and reaches the saturated specific conductivity at the ethanol concentration of 10.2 M.

In order to determine the sensitivity of these two films, the slopes of the graphs were calculated. The slope of the HCl-doped polyaniline ($-1.91\text{E-}03 \text{ Scm}^{-1}\text{M}^{-1}$) was greater than that of the CH₃COOH-doped polyaniline ($-1.1\text{E-}04 \text{ Scm}^{-1}\text{M}^{-1}$). The decrease in the specific conductivity due to the increase in the steric effect of ethanol molecules led to the reductions in H⁺-transfer and hence charges mobility. Thus, the HCl and CH₃COOH-doped polyaniline films can be used as the ethanol sensors within the ethanol concentration ranges of 1.7-8.3 M and 2.8-10.2 M, respectively. The HCl-doped polyaniline films showed the higher sensitivity than that of CH₃COOH-doped polyaniline films because of the higher degree of protonation, ethanol molecules could interact with the polyaniline chain better than CH₃COOH-doped polyaniline films.

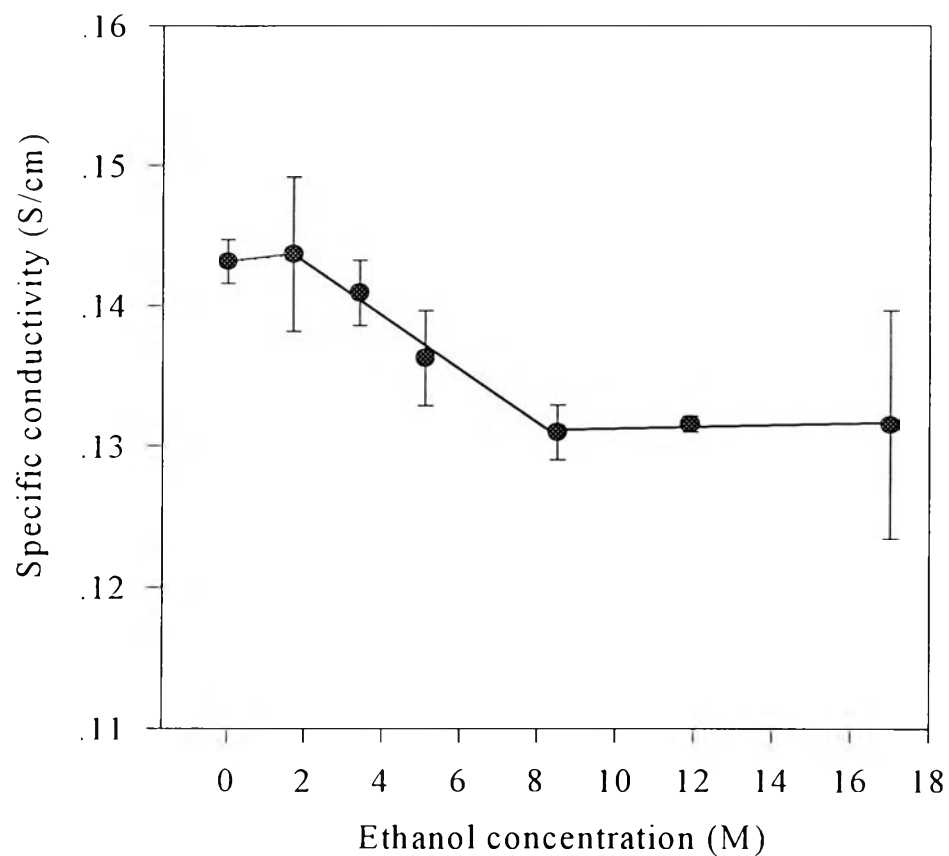


Figure 4.41 The specific conductivity of HCl-doped polyaniline films at $N_a/N_p = 9.8E+01$ when exposed to ethanol solutions at 25°C, with relative humidity between 65-70%.

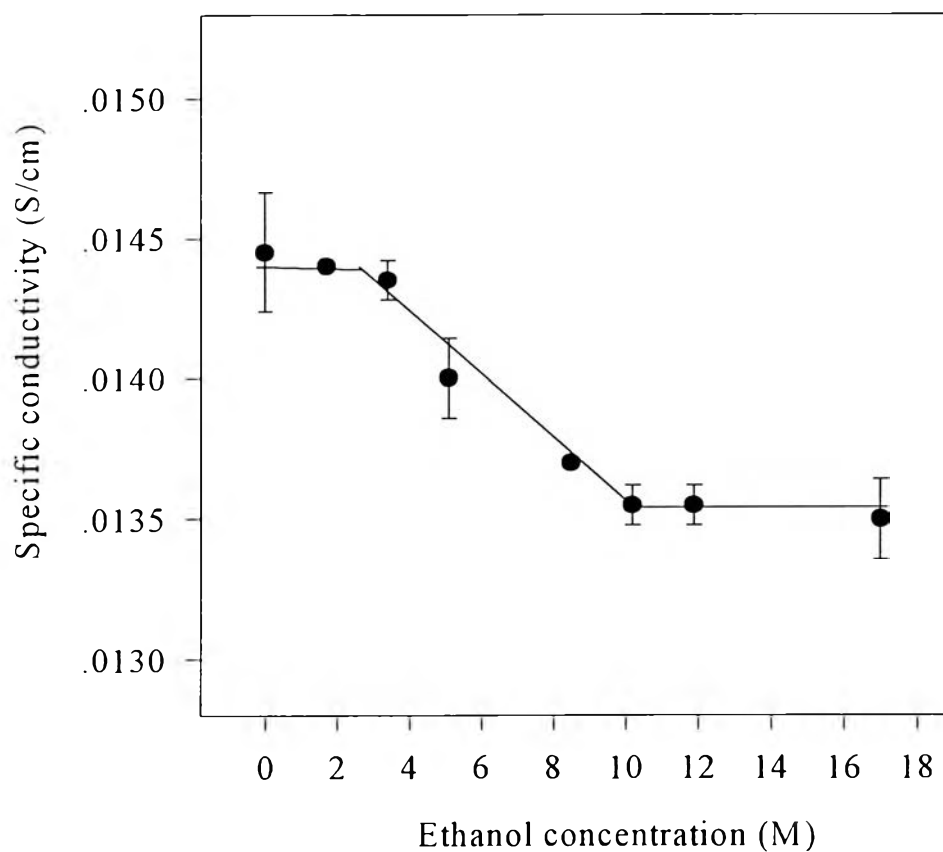
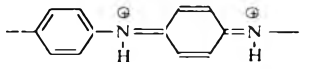


Figure 4.42 The specific conductivity of CH_3COOH -doped polyaniline films at $N_a/N_p=5.9\text{E}+03$ when exposed to ethanol solutions at 25°C , with relative humidity between 65-70%.

4.3 Characterization of Polyaniline Films after the exposure to water and 100% ethanol

The FT-IR spectra of the HCl-doped polyaniline films after the exposure to water and ethanol are compared with those films without the exposure and shown in Figure 4.41. The spectrum of HCl-doped polyaniline film when exposed to water shows 2 new absorption bands at 1493 and 1317 cm^{-1} corresponding to the stretching of benzenoid ring and vibration mode of benzenoid-benzenoid-quinoid segment (Kang *et al.*, 1998). These two absorption bands indicate that some quinoid parts in polymer chain have been protonated and the structures have changed from the quinoid structure to the benzenoid structure. The absorbance peak at 1153 cm^{-1} , which represents the broken symmetry mode of quinoid structure, , increased when the polymer films were exposed to water because of the increase in the degree of protonation. The spectrum of the CH_3COOH -doped polyaniline film after the exposure to 100% ethanol shows the identical absorption bands before the exposure indicating that ethanol molecules do not interact chemically with the polymer chains.

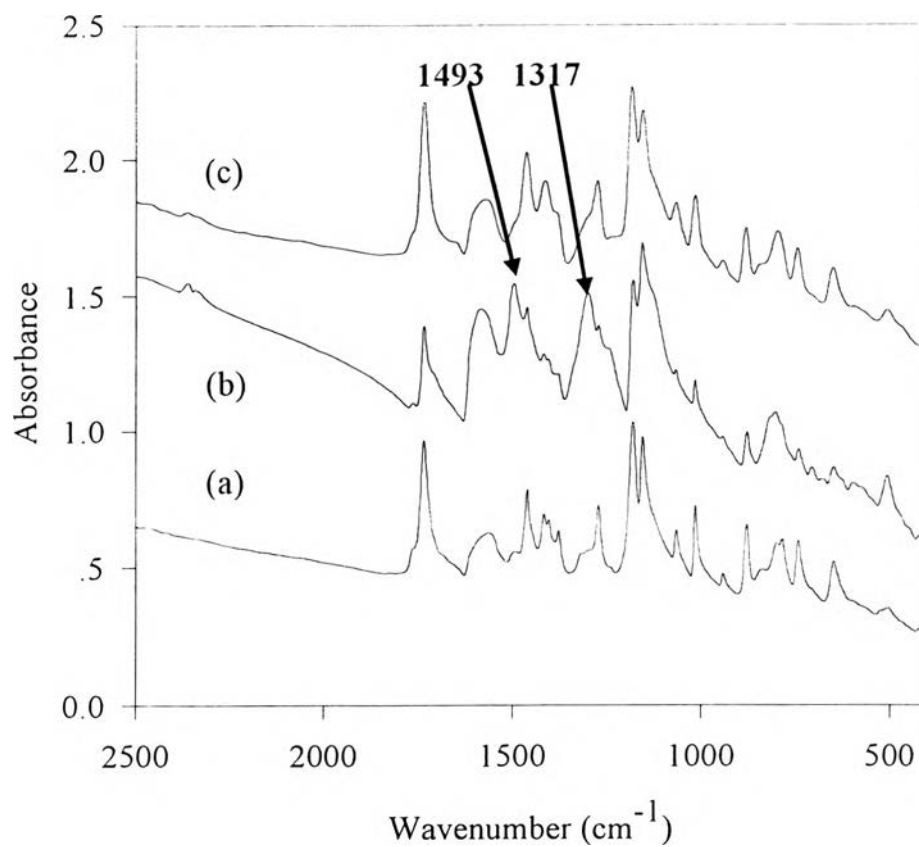


Figure 4.43 FT-IR spectra of HCl-doped polyaniline films of: (a) before the exposure to water and ethanol; (b) after the exposure to water; and (c) after the exposure to 100% ethanol.

Table 4.6 The absorption bands of FT-IR spectra of HCl-doped polyaniline films at $C_a/C_p=10:1$ ($N_a/N_p=9.8E+01$) of (a) before the exposure to water; (b) after the exposure to water; and (c) after the exposure to 100% ethanol

Wavenumber (cm^{-1})			The assignments	References
(a)	(b)	(c)		
1735	1735	1735	C=O stretching of NMP	Wei <i>et al.</i> , (1992)
1562	1563	1562	C=N stretching of quinoid ring	Milton, (1993)
-	1493	-	Stretching of Benzenoid ring	Kang <i>et al.</i> , (1998)
1459	1458	1459	Stretching of benzene ring	Milton, (1993)
-	1317	-	Vibration mode of benzenoid-benzenoid-quinoid segment	Kang <i>et al.</i> , (1998)
1271	1271	1270	C-N stretching of benzenoid ring	Milton, (1993)
1163	1163	1161	In-plane C-H bending of quinoid ring	Milton, (1993)
1153	1153	1153	Broken symmetry mode of quinoid ring	Kang <i>et al.</i> , (1998)
1065	1065	1065	Cl ⁻ substitution on meta-position	Morales <i>et al.</i> , (1997)
1014	1013	1014	Cl ⁻ substitution on ortho-position	Morales <i>et al.</i> , (1997)
878	878	878	C-H out of plane bending of 1, 2, 4-aromatic ring	Zeng and Ko, (1998)
741	741	741	C-H out of plane bending of 1, 2-aromatic ring	Kang <i>et al.</i> , (1998)